INTERNATIONAL ATOMIC ENERGY AGENCY
UNITED NATIONS EDUCATIONAL, SCIENTIFIC AND CULTURAL ORGANIZATION
INTERNATIONAL CENTRE FOR THEORETICAL PHYSICS
I.C.T.P., P.O. BOX 586, 34100 TRIESTE, ITALY, CABLE CENTRATOM TRIESTE

H4.SMR/453-27

TRAINING COLLEGE ON PHYSICS AND CHARACTERIZATION OF LASERS AND OPTICAL FIBRES

(5 February - 2 March 1990)

HIGH RESOLUTION OPTOGALVANIC SPECTROSCOPY OF ATOMIC OXYGEN

A. Sasso

Università di Napoli
Dipartimento di Scienze Fisiche
80125 Napoli

February 1990

UNIVERSITÀ DI NAPOLI

DIPARTIMENTO DI SCIENZE FISICHE

MOSTRA D'OLTREMARE PAD. 20

80125 NAPOLI – ITALY

TEL. 081 - 7253262

FAX 081 - 614508

M. INGUSCIO

L. GIANFRANI

V. MONDA

M. I. SCHIANO

A. M. TINO

A. SASSO

1. COLLISIONAL PHYSICS

   i) O-atom production

   ii) Anomalous Doppler broadening

2. FINE STRUCTURE MEASUREMENTS

3. ISOTOPE SHIFT ^{16}O, ^{17}O, ^{18}O

4. HYPERFINE STRUCTURE ^{17}O

   DIODE LASER SPECTROSCOPY

5. PROPOSAL : LASER COOLING OF ATOMIC OXYGEN BEAM.

LASER SPECTROSCOPY OF

RADIO-FREQUENCY OXYGEN PLASMA

WHY OXYGEN ?

- OXYGEN IS AN IMPORTANT ELEMENT IN MANY CHEMICAL AND PHYSICAL PROCESSES (upper atmosphere, combustion, ..)

but

OXYGEN WAS ELUSIVE TO HIGH RESOLUTION SPECTROSCOPIC INVESTIGATIONS

i) production of atomic oxygen

ii) energy level diagram :
optical transitions between
highly excited states.

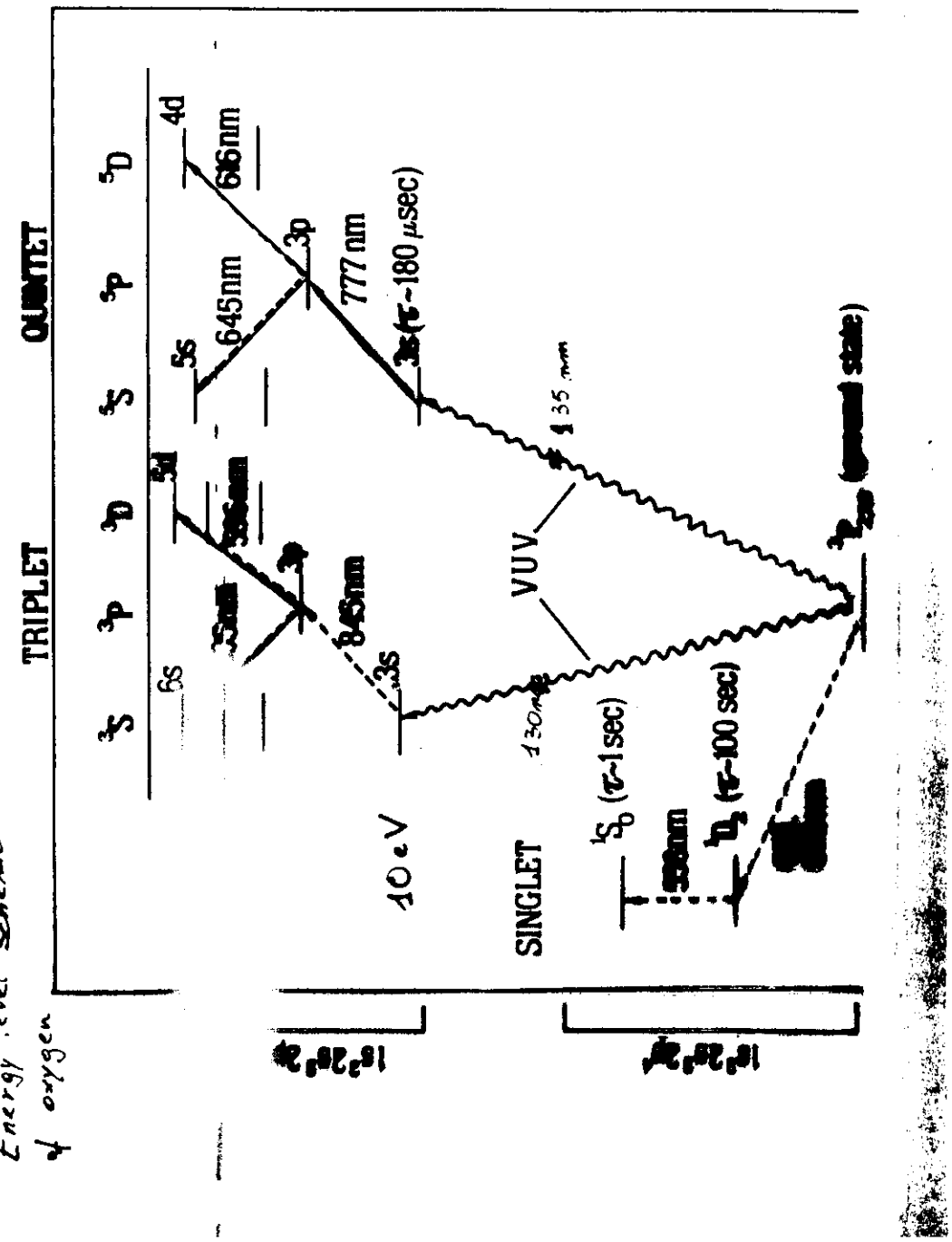

Energy level scheme of oxygen

$$P_{in} = P_{out} \cdot \frac{1}{T_2}$$

Intracavity Spectroscopy

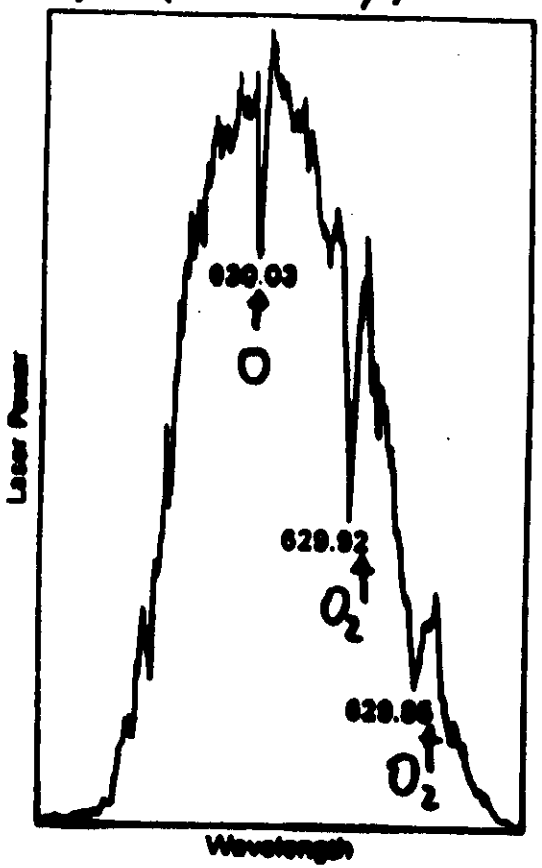

Fig. 1. Intracavity spectrum of the O($^3P_2$) tion at 630.03 nm, centered in the laser's g pair of O_2 lines at 629.92 and 629.85 nm is w pumping power is about twice threshold (P° element is a tuning wedge.

(^1D) transi- profile. A ent. The The tuning

TWO PHOTON IN FLAMES

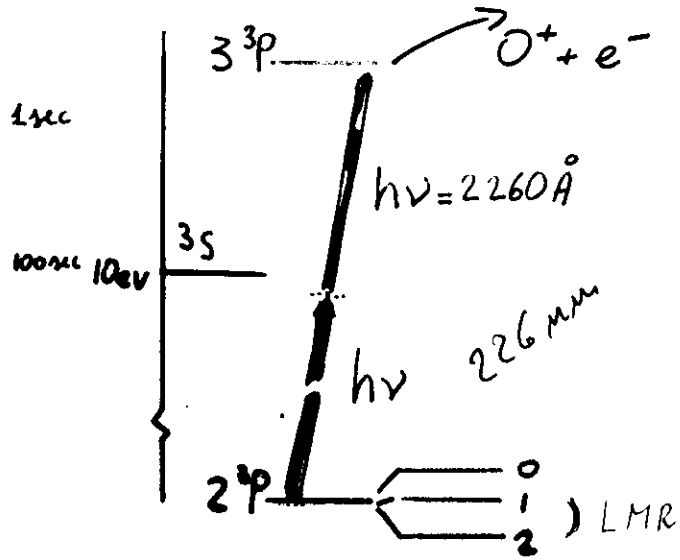

Goldsmith J Chem Phys 78, 1610 (83)

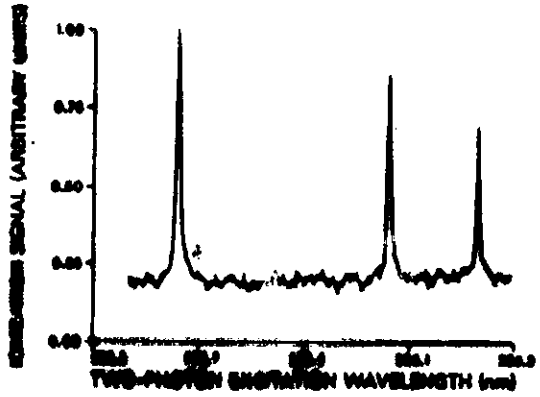

FIG. 1. Ionization signal from atomic oxygen recorded in an atmospheric pressure stoichiometric hydrogen/oxygen/argon flame. There are three peaks because of fine-structure splitting of the 3^3P state.

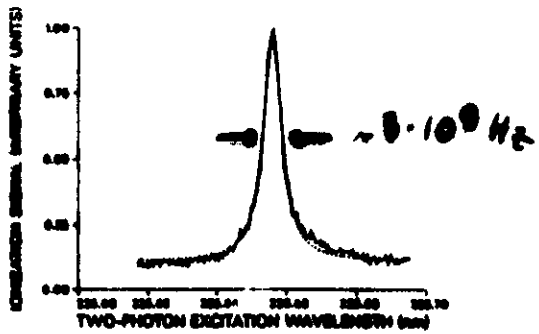

TWO PHOTON
FOURIER TRANSFORM LIMITED
PULSED LASER LINEWIDTH

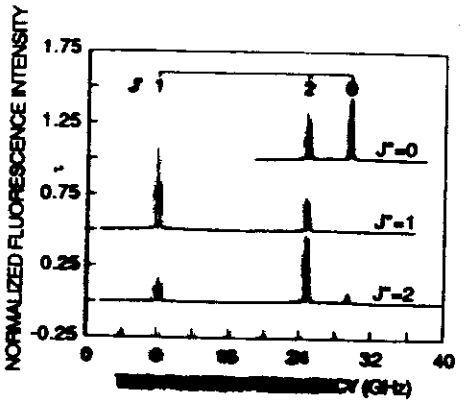

FIG. 1. Doppler-free spectra for the $3p\,^3P_{J'} \leftarrow 2p\,^3P_{J''}$ two-photon transitions in atomic oxygen. The final two-photon excitation is monitored using fluorescence from the $3p\,^3P_{J'} \rightarrow 3s\,^3S^0_1$ transitions at 845 nm, proportional to the square of the laser intensity. Doppler-free absorption forms a broad pedestal underneath each peak. Each spectrum has the same integrated area. The middle and top spectra are displaced from the bottom one by 0.5 and 1.0 vertical units, respectively.

TABLE I. Experimental and theoretical (in parentheses, from Ref. 5) integrated two-photon cross sections for the $3p\,^3P_{J'} \leftarrow 2p\,^3P_{J''}$ transition in atomic oxygen.

		$\sigma^{(2)}(J' \leftarrow J'')$		
J''	J'	Absolute (10^{-36} cm^4)[a]		Relative[b]
2	2	13.2	(9.42)	0.786 ± 0.077(0.714)
2	1	3.63	(2.64)	0.194 ± 0.043(0.198)
2	0	1.87	(1.16)	0.100 ± 0.040(0.088)
1	2	6.98	(4.34)	0.373 ± 0.067(0.329)
1	1	11.7	(8.86)	0.627 ± 0.067(0.671)
1	0	0	(0)	0 (0)
0	2	9.01	(5.79)	0.482 ± 0.045(0.439)
0	1	0	(0)	0 (0)
0	0	9.69	(7.61)	0.518 ± 0.045(0.561)

[a] These numbers must be multiplied by a line-shape factor $g(\omega - \omega_{J'})$ to get the effective cross section at any given two-photon radiation frequency, ω. If the line-shape function is a 300-K Doppler profile $g(0) = 4.86 \times 10^{-11}$ sec.
[b] Experimental error limits are $\pm 1\sigma$, where σ is the sample standard deviation.

BISCHEL et al. Phy. Rev. A 36, 3497 (1987)

LASER DIAGNOSTIC OF OXYGEN PLASMA:

a) necessary to perform spectroscopic investigation

i) source of informations on the collisional processes governing the O-atoms formation.

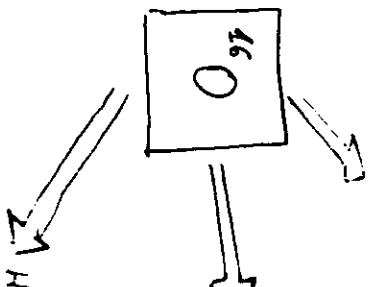

gas inlet (O_2 + noble gas)

LASER BEAM

$\nu \sim 60$ MHz

$P \sim 50$ Watt

radio frequency Oscillator

current feed-back

to lock-in

OG signal

Power supply

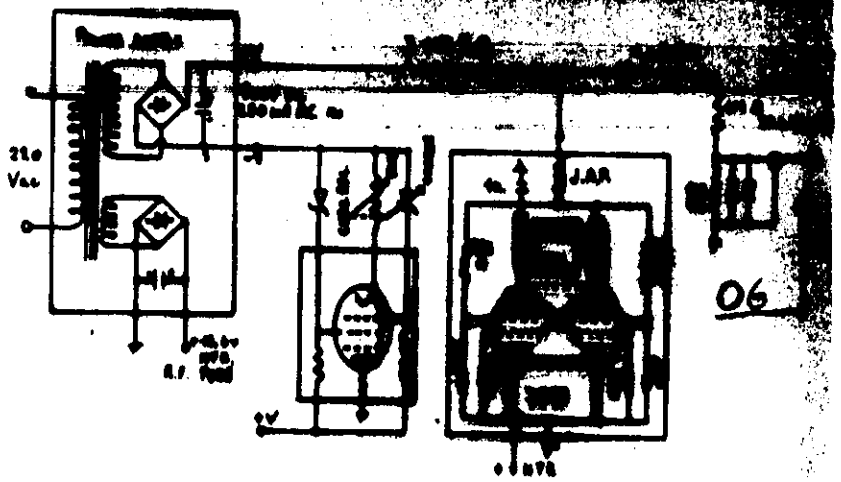

A. Sasso, G. Tino, M. Inguscio, N. Beverini, M. Francone

Nuovo Cimento D 10, 941 (1988)

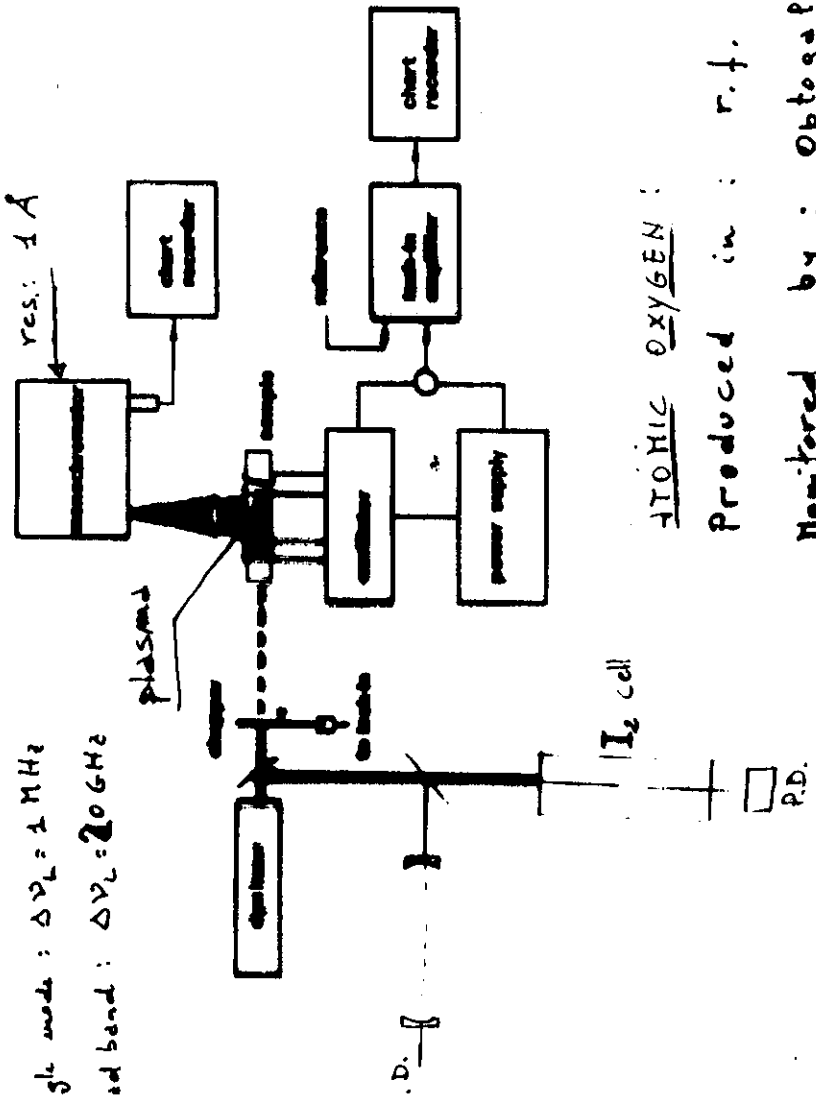

single mode: $\Delta\nu_L = 1$ MHz

wide band: $\Delta\nu_L = 20$ GHz

ATOMIC OXYGEN:

Produced in: r.f. discharge

Monitored by: optogalvanic and fluorescence detection.

$Ne - O_2$

A. Sasso, G. Minguzzi, T. ... Schisano
G. Fino and M. [illegible] J. Opt. Soc. Am B
2, 241 (85)

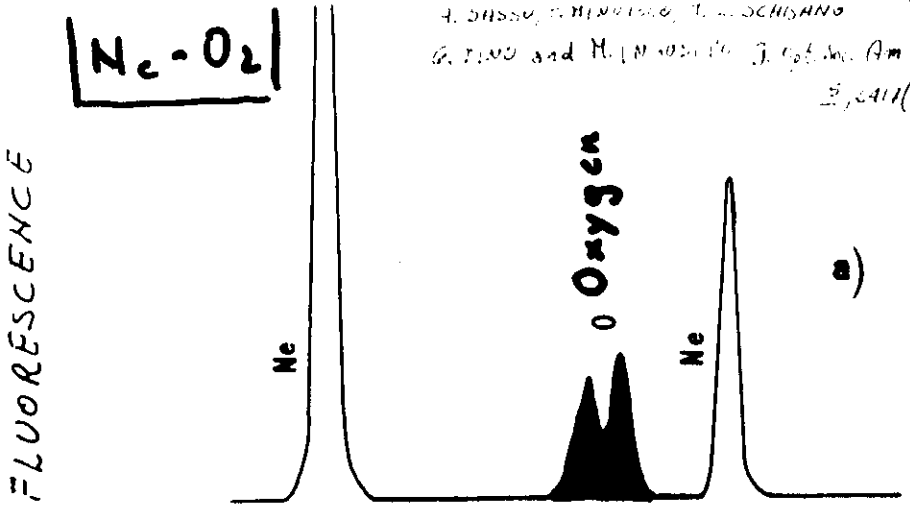

P_{O_2} = 0.2 Torr

P_{Ne} = 10 Torr

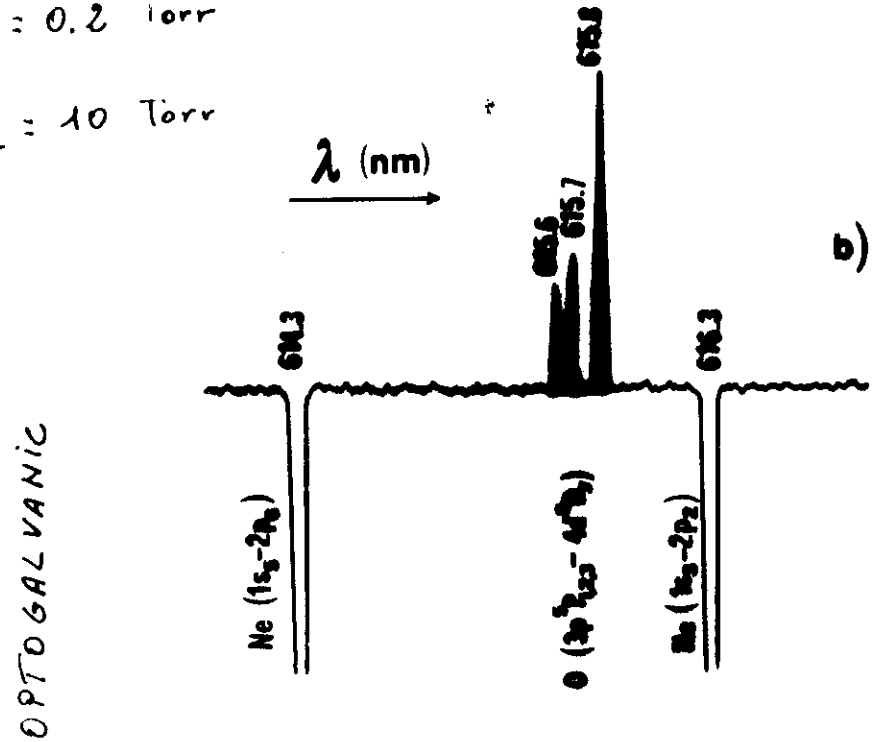

$Ne^*(1s_5) \rightleftharpoons Ne^*(^3P_2)$

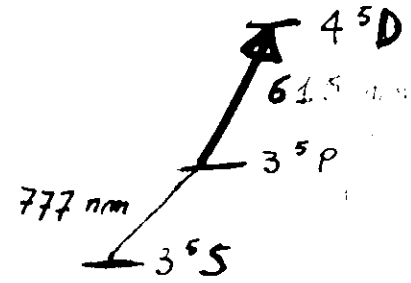

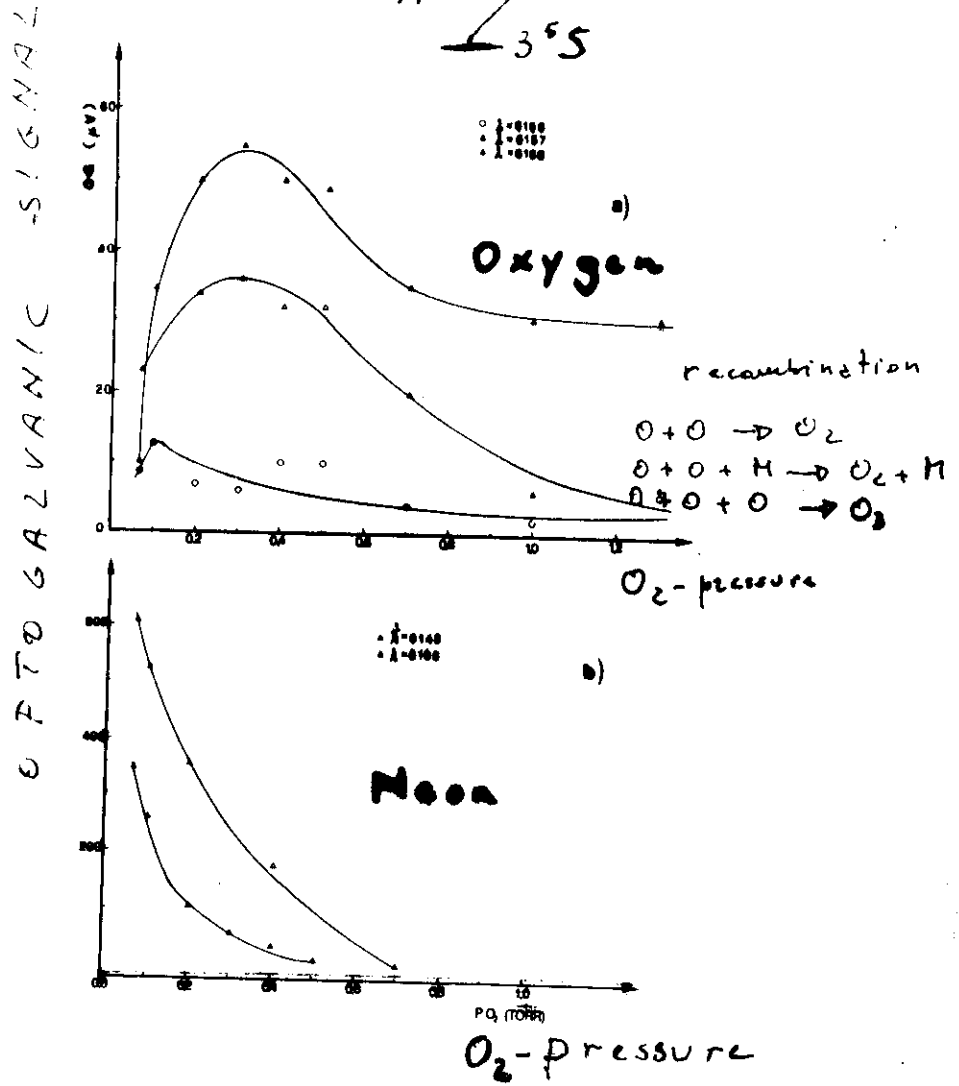

The decrease of Ne, OG signals can be explained - terms of the reaction

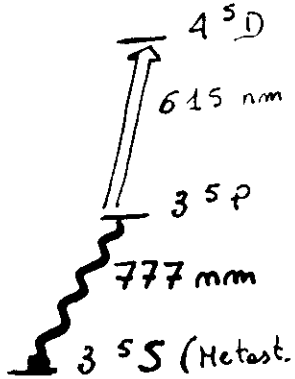

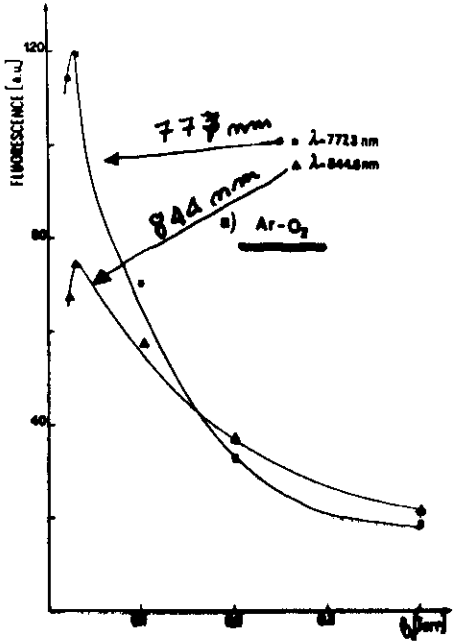

FLUORESCENCE

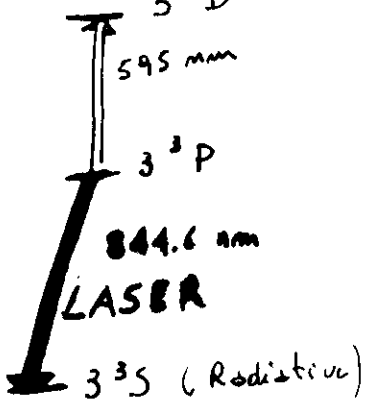

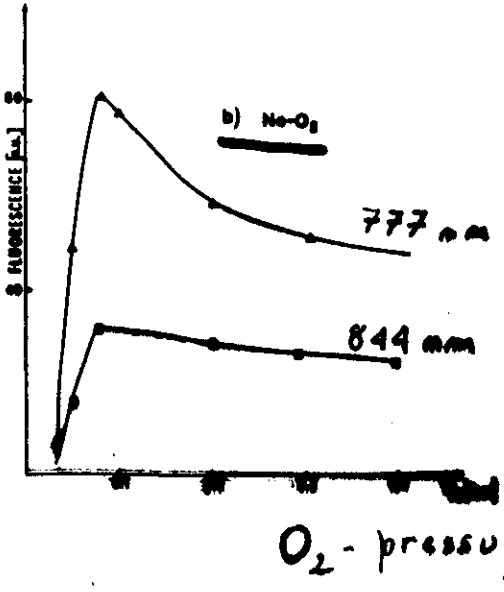

W.R. Bennet, Jr., W.L. Faust, R.A. McFarlane, C.K.N. Patel
P.R.L. 8, 470 (1962)

$$\frac{d[Ne^*]}{dt} = Zn_e[Ne] - \alpha[O_2][Ne^*] - w[Ne^*] - T[Ne^*]^2, \quad (4)$$

$$\frac{d[O^*]}{dt} = \alpha[O_2][Ne^*] - \beta[O_2][O^*] - \frac{[O^*]}{\tau_{O^*}} - D_{dif}[O^*], \quad (5)$$

$$\frac{d[O]}{dt} = \frac{[O^*]}{\tau_{O^*}} + 3\beta[O_2][O^*] + \alpha[O_2][Ne^*] - \gamma[Ne^*][O]^2.$$

$$[O^*] = \frac{Z\alpha[O_2][Ne]n_e}{\alpha\beta[O_2]^2 + \left(\frac{\alpha}{\tau_{O^*}} + w\beta + D_{dif}\alpha\right)[O_2] + \frac{w}{\tau_{O^*}} + D_{dif}w} \quad (7)$$

TABLE II

[illegible] in the kinetic model.

1	[illegible]	[illegible]	1
2	[illegible]	[illegible]	2
3	[illegible]	[illegible]	3
4	[illegible]	[illegible]	4
5	[illegible]	[illegible]	5
6	[illegible]	[illegible]	6
7	[illegible]	[illegible]	7
8	[illegible]	[illegible]	8
9	[illegible]	[illegible]	9
10	[illegible]	[illegible]	10
11	[illegible]	[illegible]	11
12	[illegible]	[illegible]	12
13	[illegible]	[illegible]	13
14	[illegible]	[illegible]	14
15	[illegible]	[illegible]	15
16	[illegible]	[illegible]	16
17	[illegible]	[illegible]	17
18	[illegible]	[illegible]	18
19	[illegible]	[illegible]	19
20	[illegible]	[illegible]	20
21	[illegible]	[illegible]	21
22	[illegible]	[illegible]	22
23	[illegible]	[illegible]	23

ATOMIC OXYGEN FORMATION

- Pure O_2 - discharge

  Electron - impact dissociation

  $$e^- + O_2 \rightarrow e^- + O^* + O^*$$

- O_2 - noble gases mixture (X)

  i) Metastable atoms (X) are efficiently produced and represent a reservoir of energy:

  $$X + e^-_{fast} \rightarrow X^* + e^-_{slow}$$

  - $X^* + O_2 \rightarrow X + O_2^+ + e^-$ Penning ionization
  - : $X^* + O_2 \rightarrow [X^+ O_2^-]$
  - :: $X^* + O_2 \rightarrow X + O + O^*$

  For He^*, Ne^* → P. I.

  For Ar^*, Kr^*, Xe^* → Quasi-mole

- Ne - O_2 mixtures

$$Ne^*(^3P_{0,2}) + O_2 \rightarrow Ne(^3S_0) + O_2^+(a^4\Pi_u) + e^-$$

$$O_2^+ + e^- \rightarrow O(2^3P) + O^*(n^3P, n^5P)$$

resonant dissociative recombination

- Ar - O_2 mixtures

$$Ar^*(^3P_{0,2}) + O_2 \rightarrow (Ar^+ O_2^-) \rightarrow$$

$$\rightarrow Ar(^1S_0) + O^*(2^1S, 2^1D) + O(2^3P) + \underline{\Delta E}$$

ΔE : energy defect → kinetic energy

→ warm atoms

$$O^*_{warm}(2^1S, 2^1D) + e^- \xrightarrow{?} O^*_{warm}(n^3P, n^3P) + e^-$$

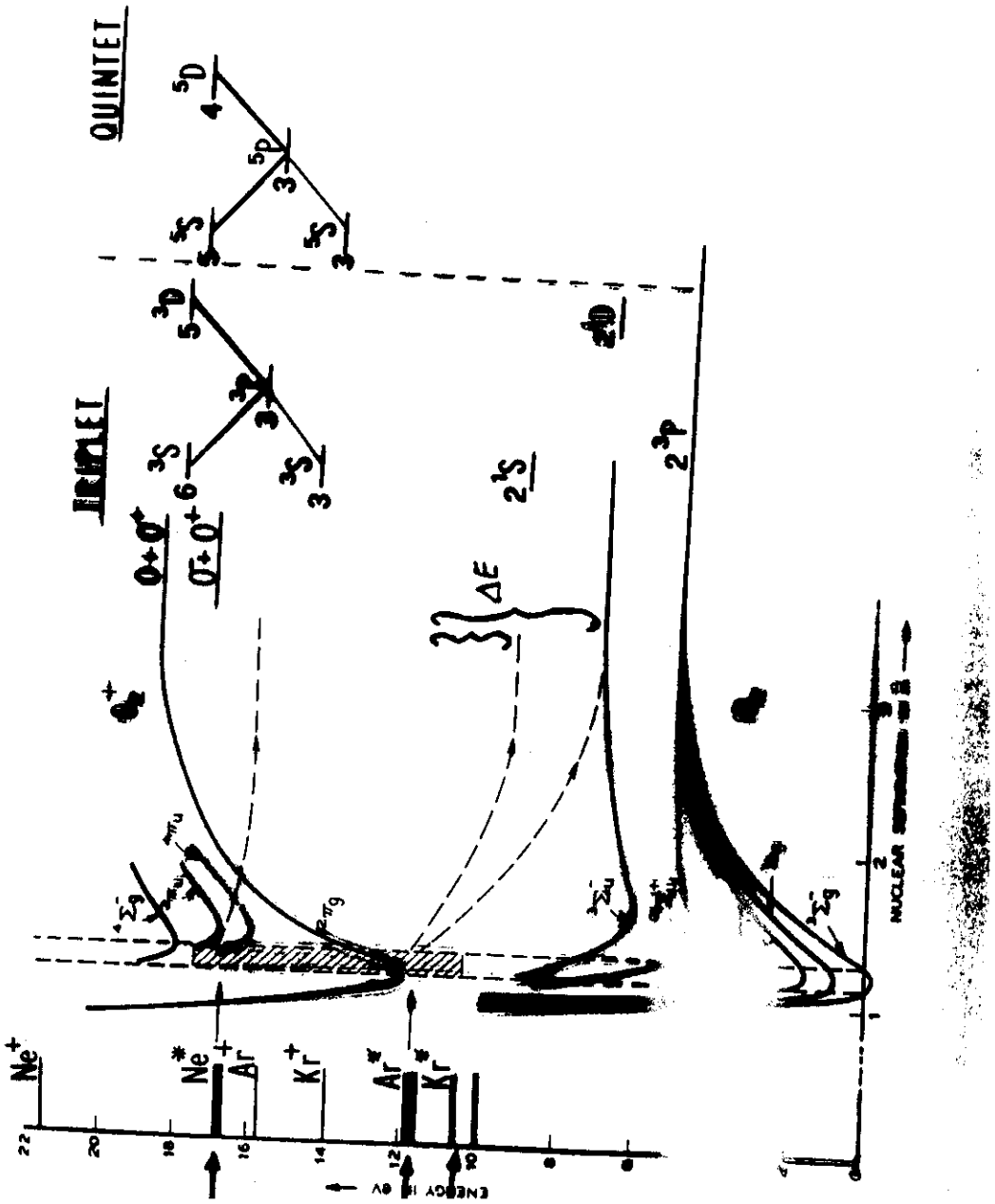

LINESHAPES OF OPTICAL TRANSITIONS IN R.F. DISCHARGE

DOPPLER-BROADENING IS DOMINANT AT OUR PRESSURES ($p = 0.1 \div 10$ Torr)

$$\Delta\nu_D = 7.16 \cdot 10^{-7}\, \nu_0 \sqrt{\frac{T}{M}}$$

From $\Delta\nu_D$ measurements

⇓

Temperature of the discharge

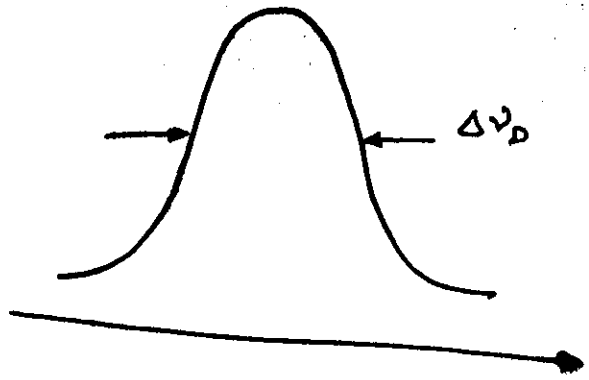

Quintet transitions:

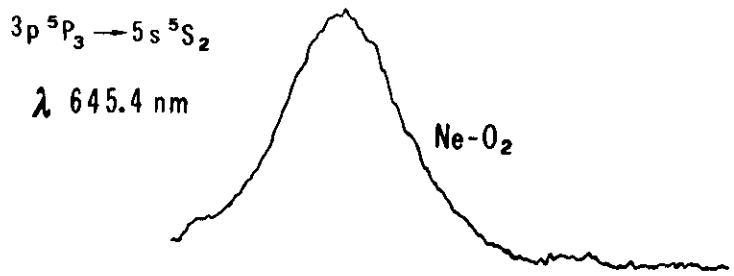

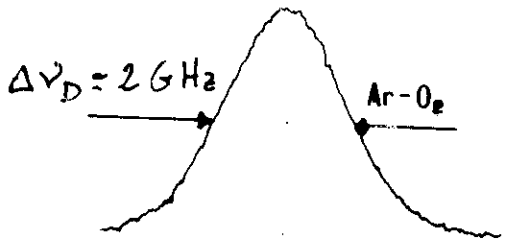

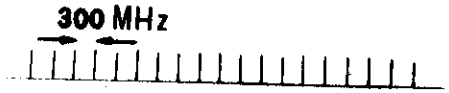

"Normal" Doppler width

$\Delta\nu_D = 2\,GHz \Longleftrightarrow T = 570\,K$

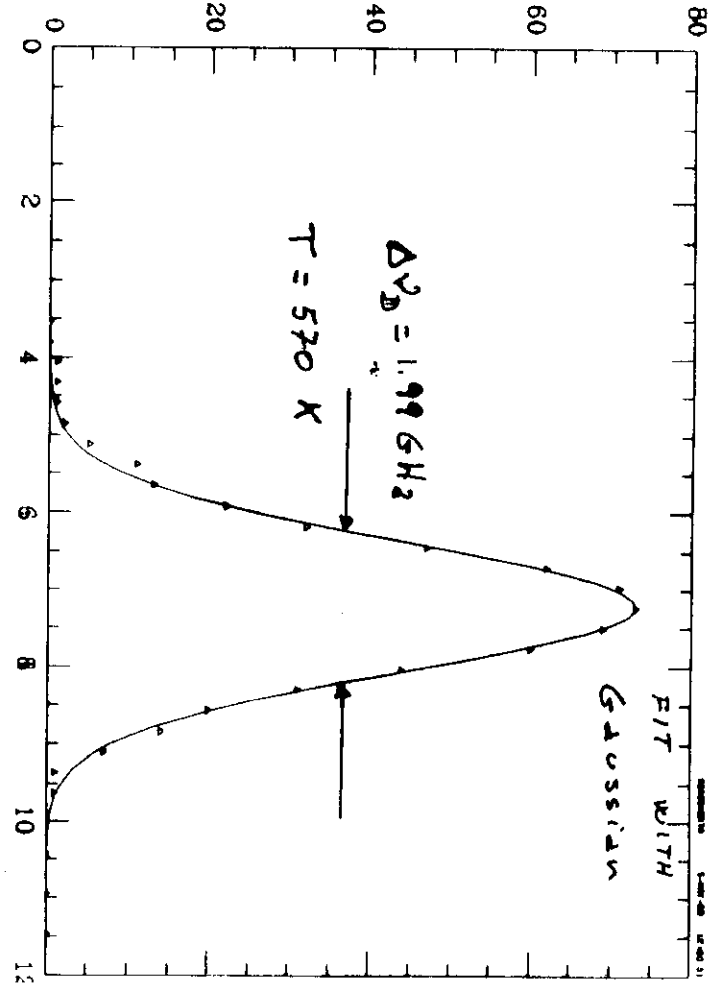

Ne-O_2: pure Doppler broadening

TRIPLET TRANSITION

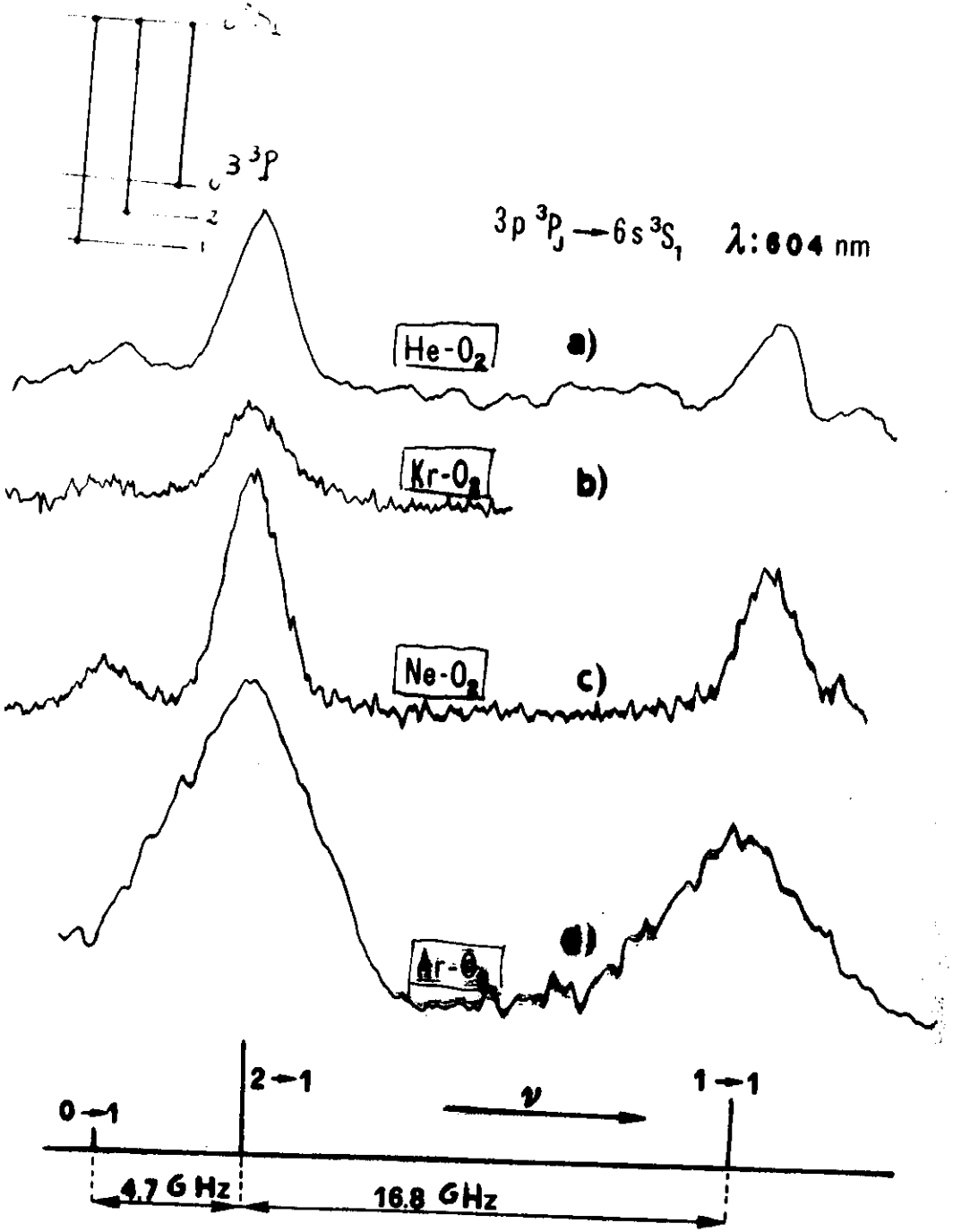

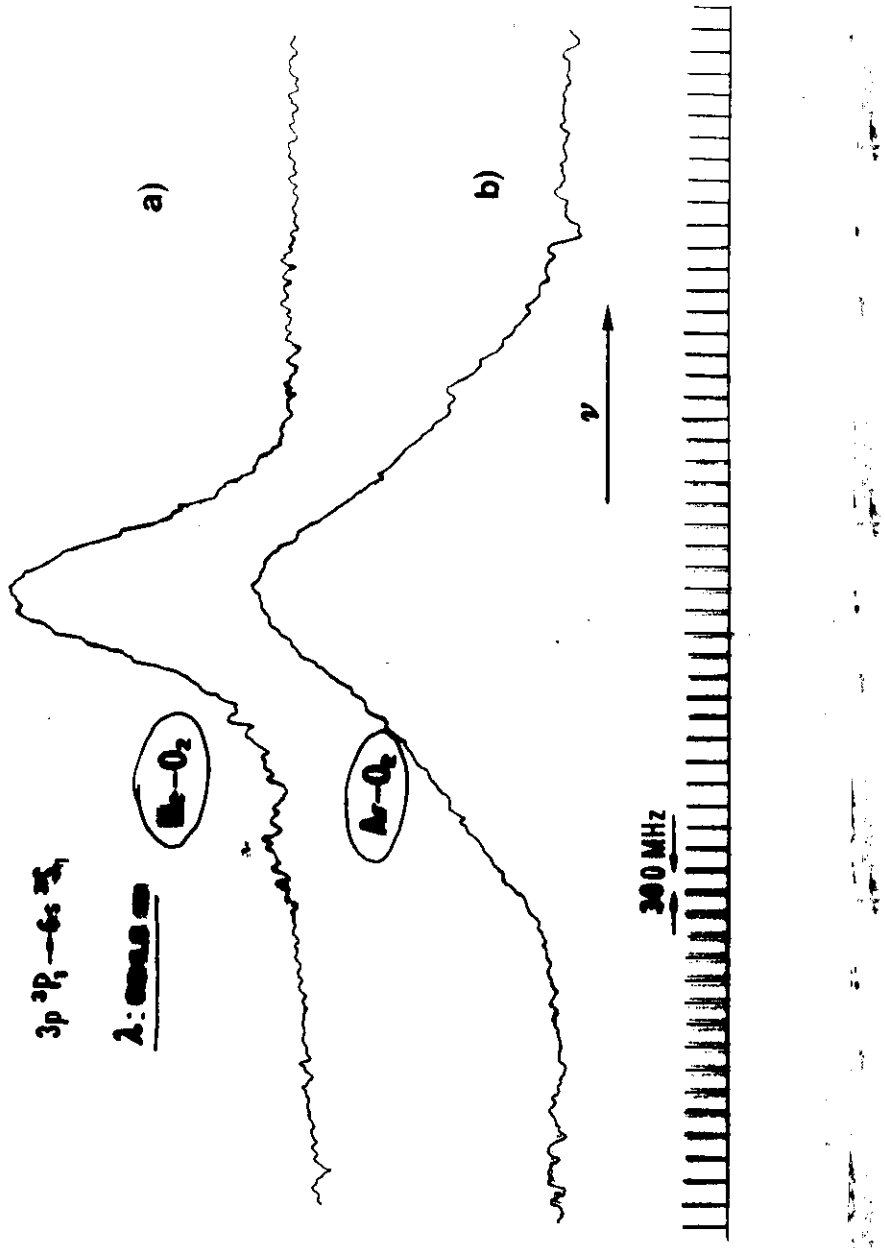

Ar - O_2 : anomalous broadening

exp. lineshapes fitted with two Gaussians

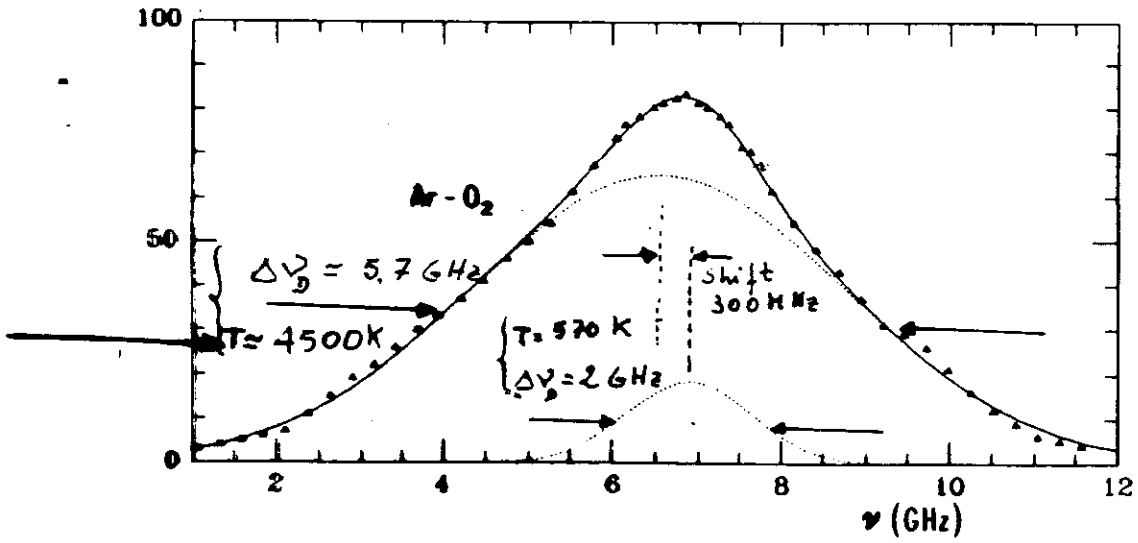

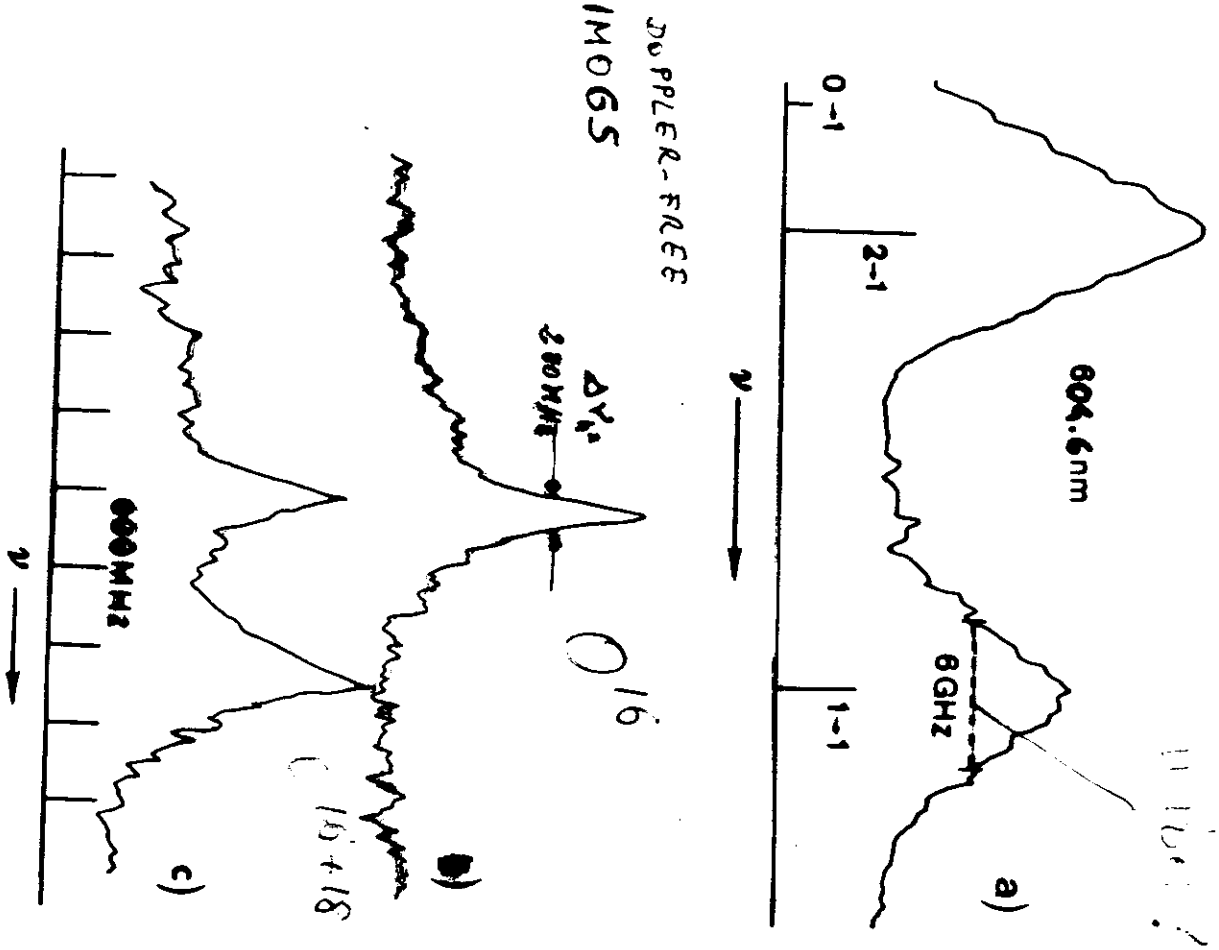

Triplet

DOPPLER-LIMITED
5.7 GHz
160 MHz
POLARIZATION SPECTROSCOPY
ν

$^3P_{1,2,0} \rightarrow {}^3D_j$
λ = 5959 Å
(a
Ar - O_2
(b
He - O_2
I_2
(c
0
20
ν(cm
$5\,{}^3D_{3,2,1}$
$3\,{}^3P$

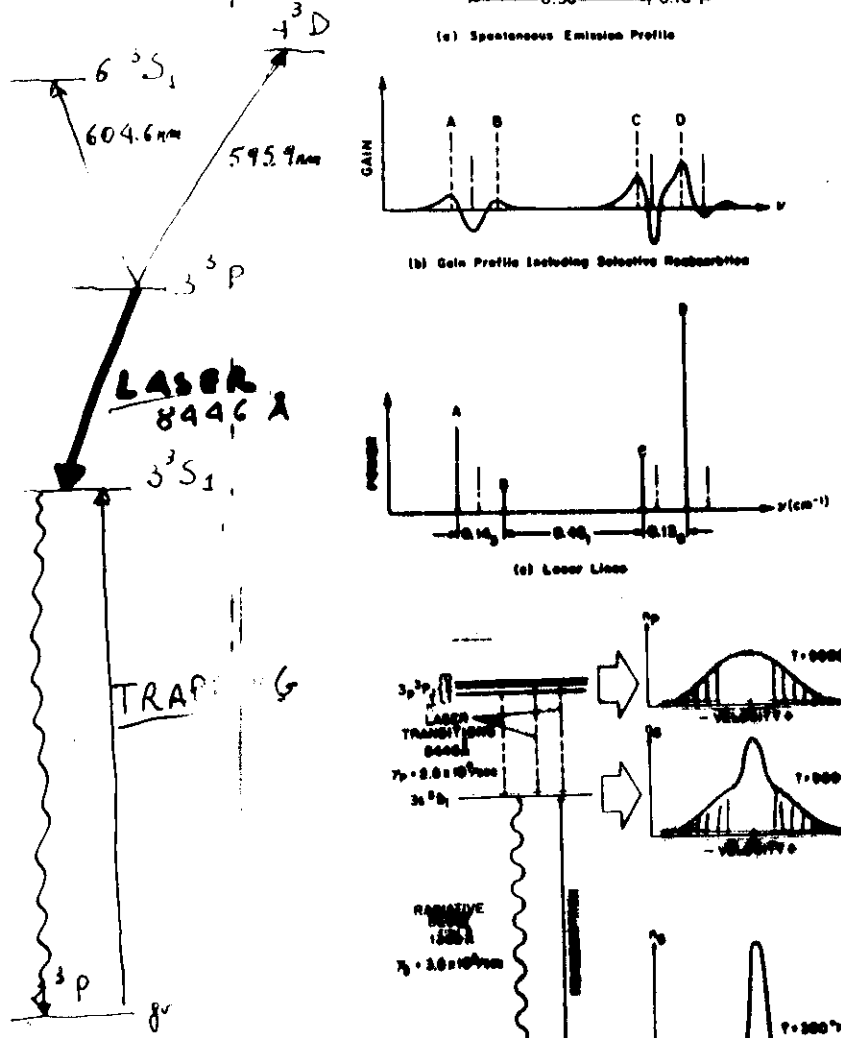

FIG. 2. (a) Relevant atomic-oxygen energy levels, and (b) corresponding velocity distributions, showing selective reabsorption.

Feld, Feldman and Javan
Phys. Rev. A7, 952 (1973)

FLUORESC.

O_2 . 1 Torr
Ne 10 Torr

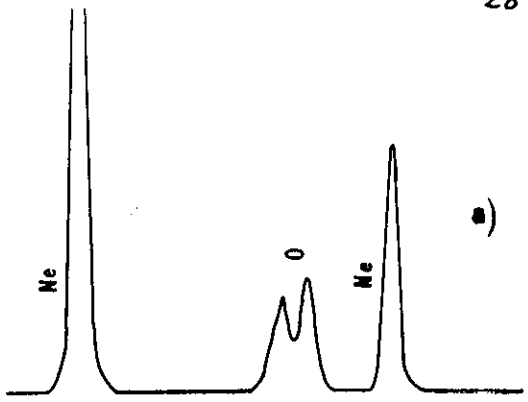

O. G.

MULTIMODE
LASER

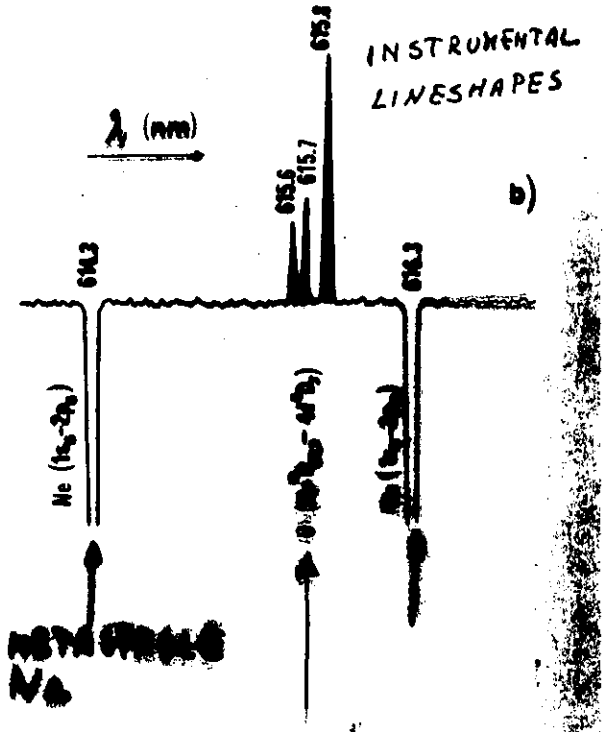

FINE STRUCTURE OF THE TRANSITION
M.I., P. MINUTOLO, A. SASSO, G. TINO : Phys. Rev. A37, 4056 (1988)

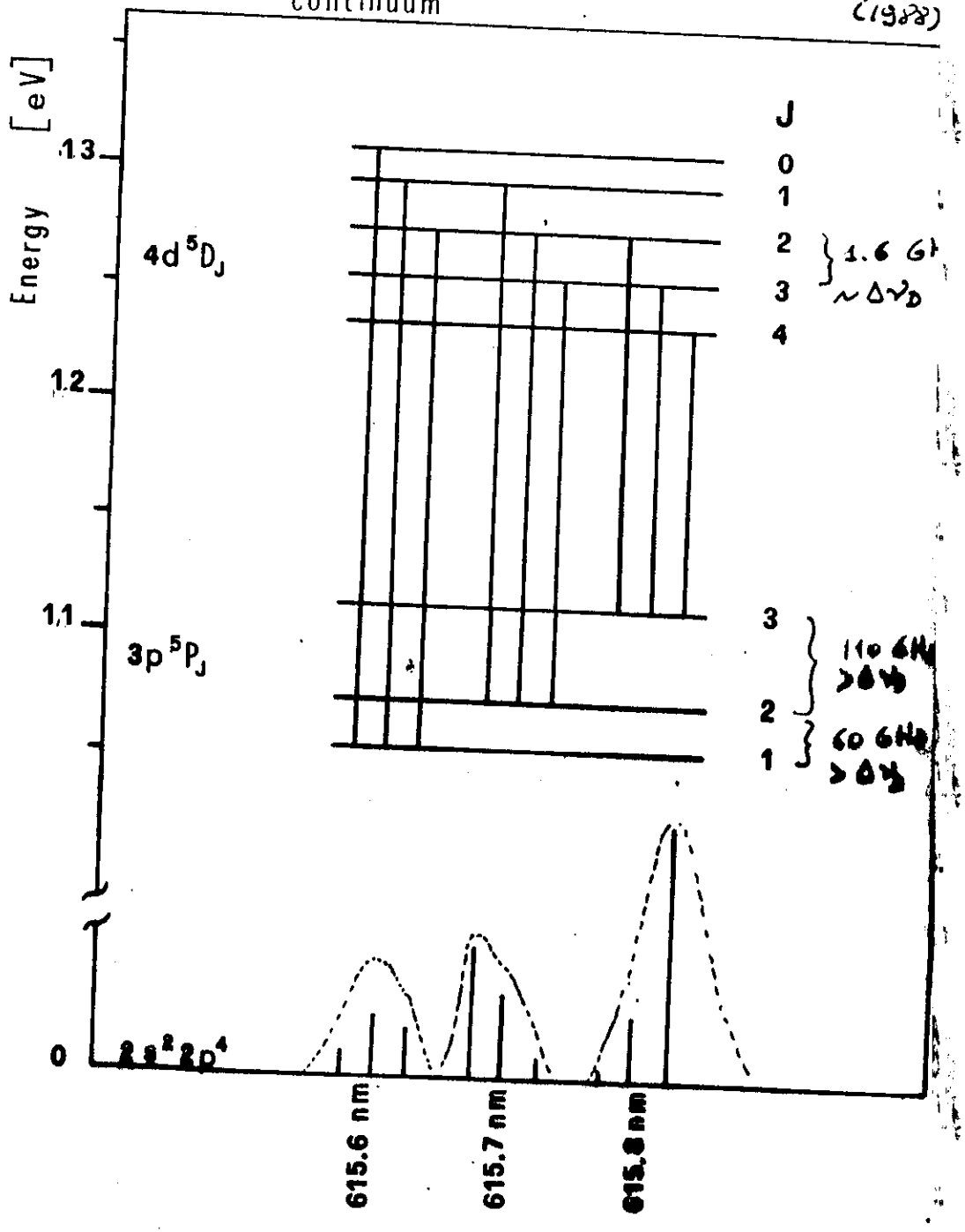

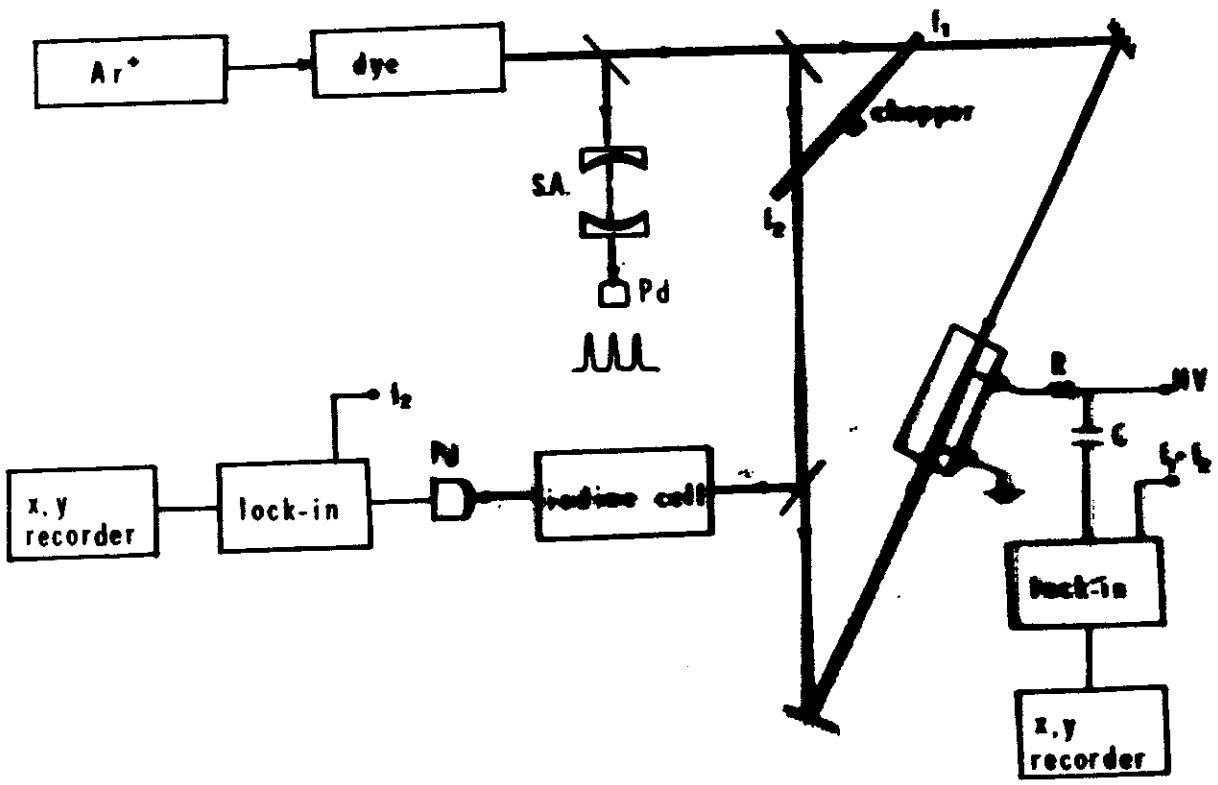

Fig. 2

APPARATUS FOR HIGH RESOLUTION.

FIT TO THE SUM OF THREE [illegible] PROFILES

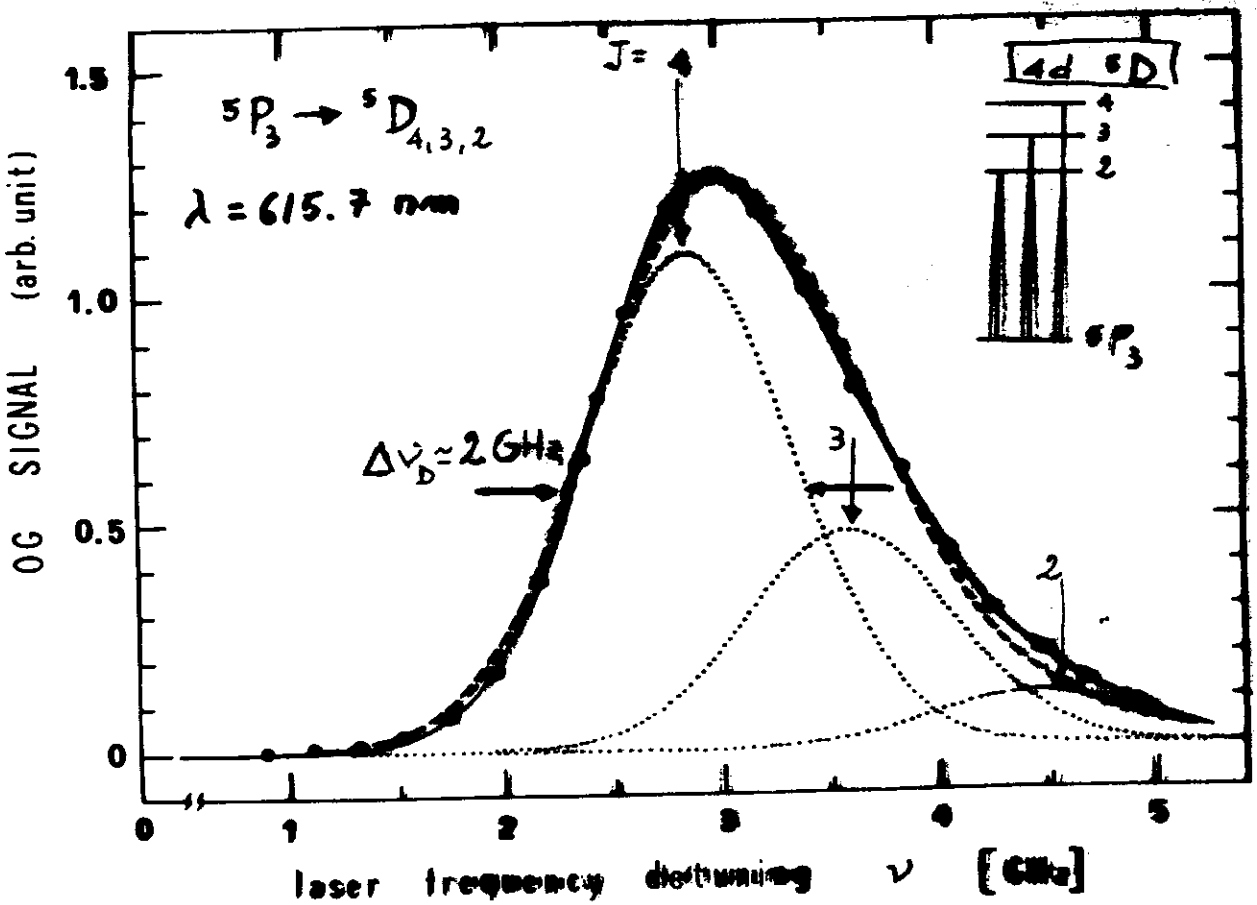

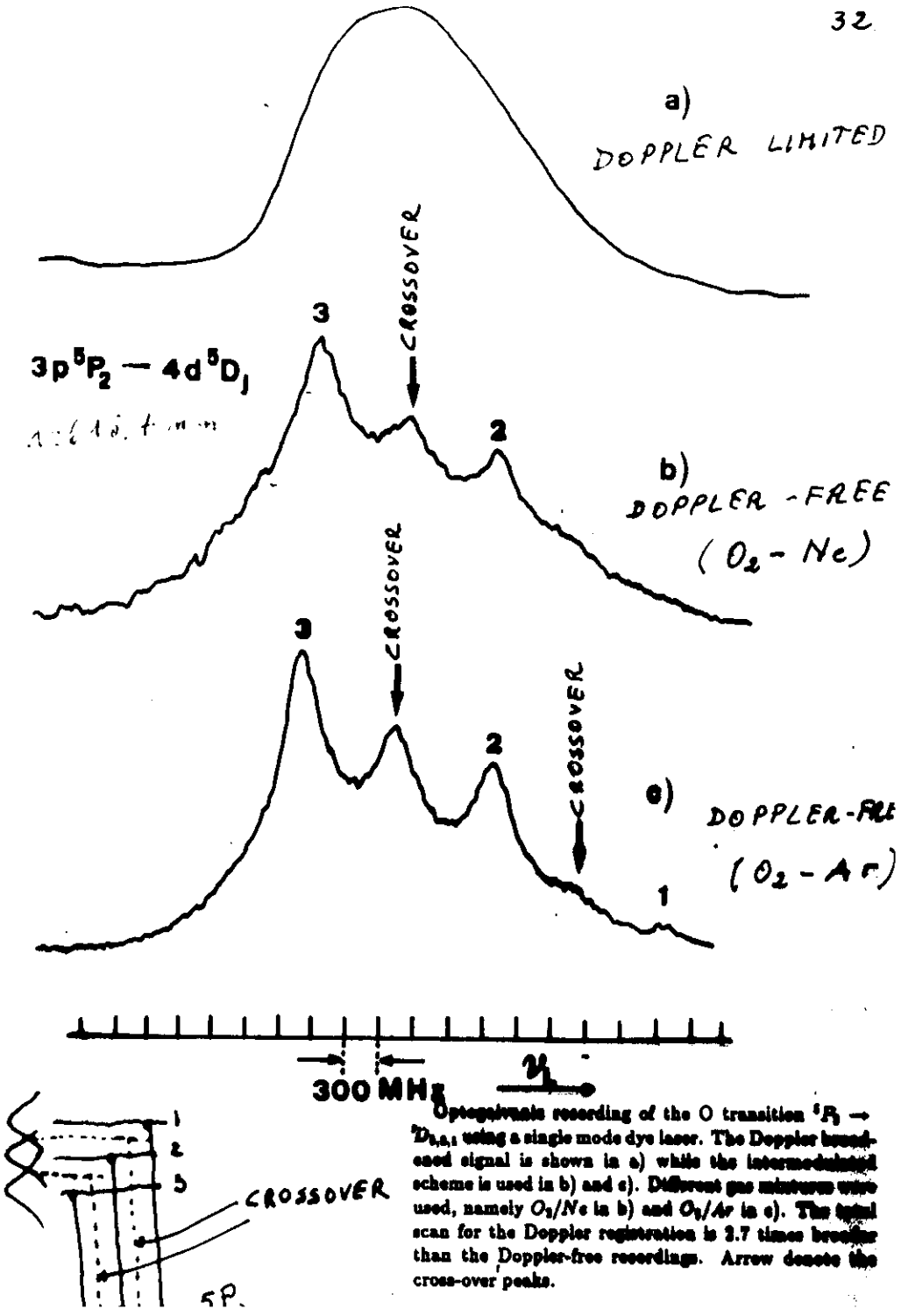

Optogalvanic recording of the O transition $^5P_3 \rightarrow {}^5D_{3,2,1}$ using a single mode dye laser. The Doppler broadened signal is shown in a) while the intermodulated scheme is used in b) and c). Different gas mixtures were used, namely O_2/Ne in b) and O_2/Ar in c). The total scan for the Doppler registration is 2.7 times broader than the Doppler-free recordings. Arrow denote the cross-over peaks.

K. ERNST, P. MINUTOLO, A. SASSO, G. TINO, M. I.: Opt. Lett. 14, 554 (89)

O
645.6 nm
$3^5P_3 - 5^5S_2$

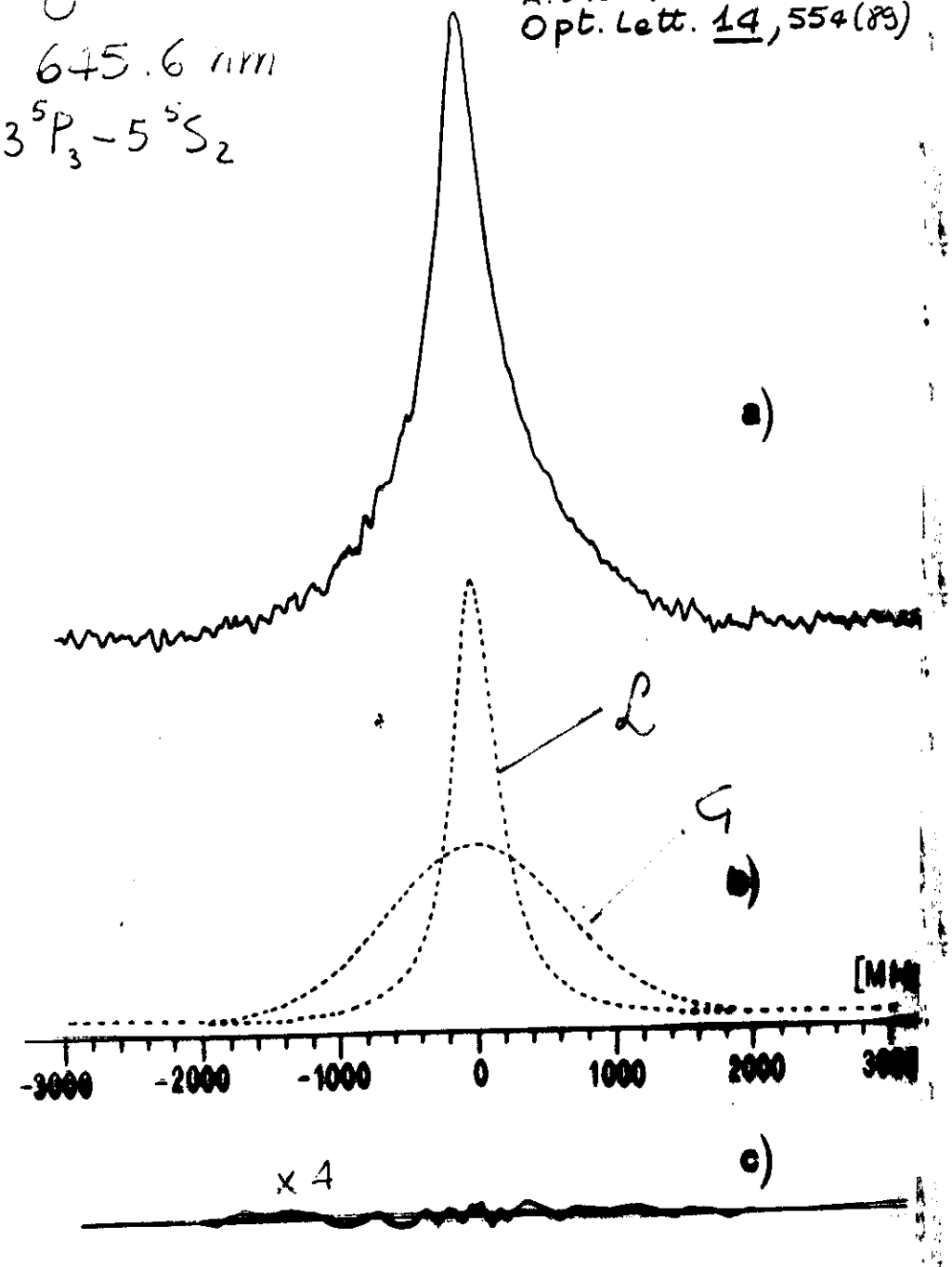

$$A\left[\frac{\gamma^2/4}{\gamma^2/4+(\nu-\nu_0)^2}+C\exp\left(-\frac{\nu-\nu_0}{\delta\nu_D}\right)^2\right]\times\zeta$$

$$C=2\sqrt{\pi\ln 2}\,\frac{\Gamma\gamma}{\delta\Delta_D}$$

O_2/Ar (.1/5 Torr)

$\Delta\nu_D = 2$ GHz (520 °K)

$\gamma=\Delta\nu_{hom}=$ **386 MHz** (FWHM)

$C = 0.39$

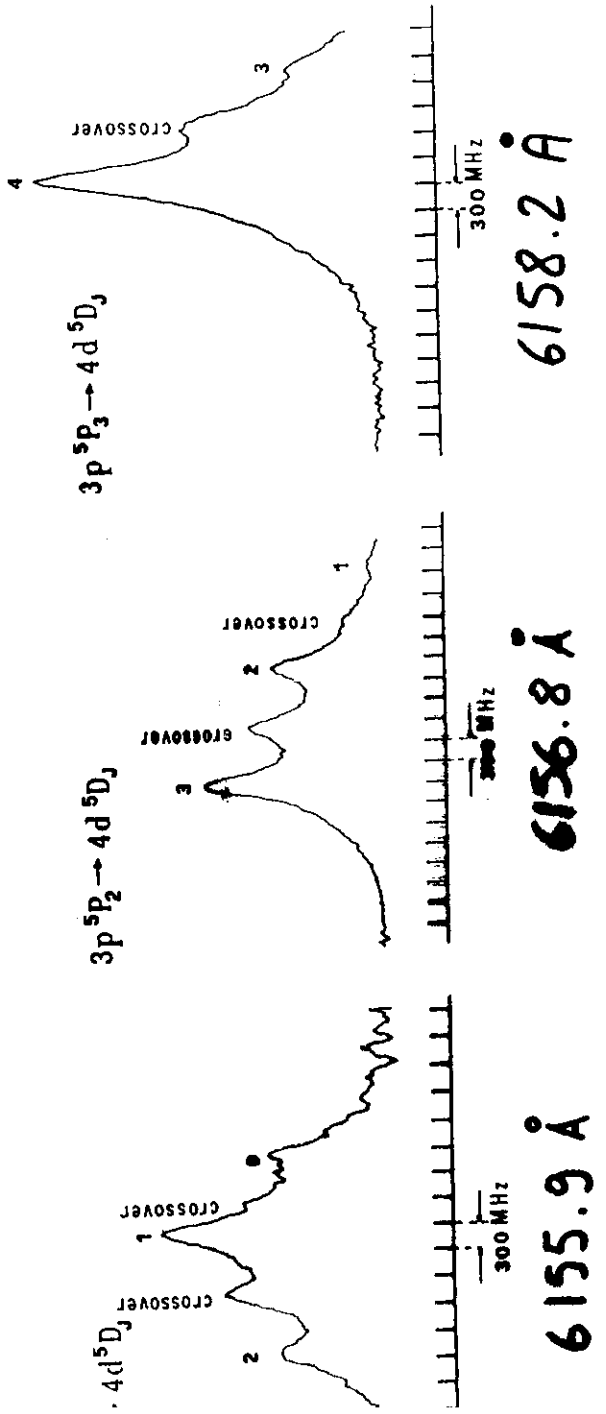

[2] H. Hinderson et al. Phys. Rev. A 33, 4056 (1986)
[2] J.J. Champeau et al. J. Phys. B 8, 728 (1975)
[3] Kas. Eriksson et al Ann. Fysik 24, 549 (1963)

Table I

Δ_{ij}	Our results (MHz)[4]	Ref.[2] (MHz)	Ref[3] (MHz)
Δ_{0-1}	735(20)	786(51)	720(200)
Δ_{1-2}	1360(20)	1416(24)	1469(200)
Δ_{2-3}	1594(20)	1680(24))	1769(200)
Δ_{3-4}	1362(20)	1407(30)	1229(200)

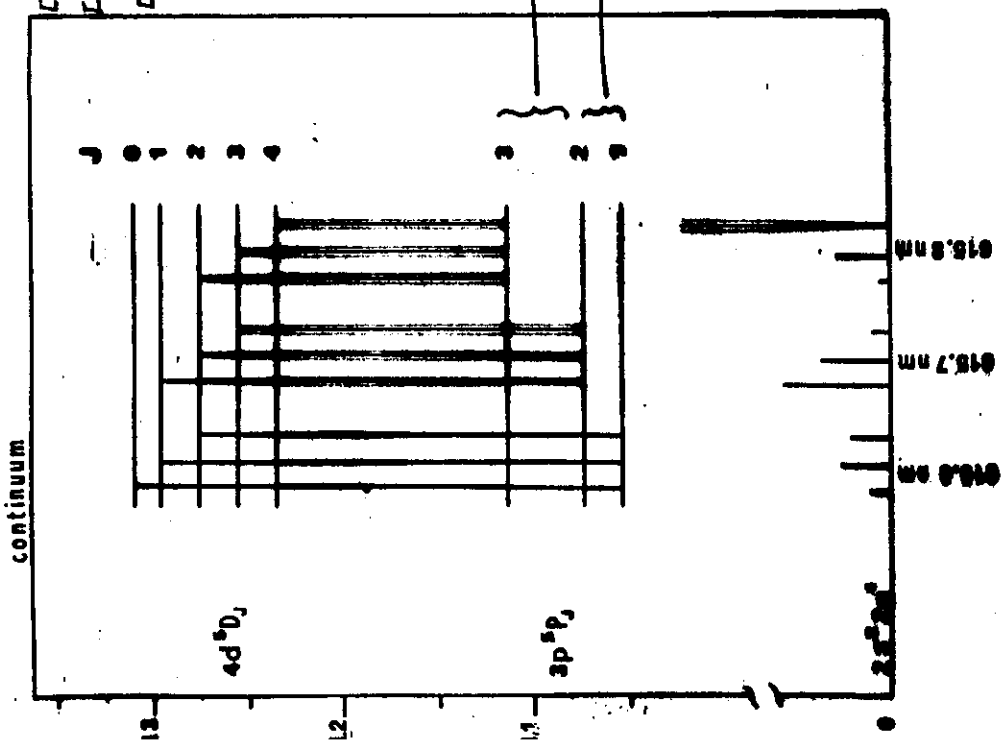

TABLE I. Fine structure splittings in the atomic oxygen $2p^3(4S^0)4d\ ^5D_{4,3,2,1,0}$ levels as obtained from sub-Doppler spectroscopy. For comparison the data deduced in conventional spectroscopy are reported.

FINE STRUCTURE: THEORY

$$H = \sum_i \left[\frac{p_i^2}{2m} - \frac{Ze^2}{r_i} + U_i(\vec{r}_i) \right] + \sum_{i<j} \left[\frac{e^2}{r_{ij}} - U_i(\vec{r}_i) \right] + \sum_i a(\vec{r}_i)\, \vec{l}_i \cdot \vec{s}_i \qquad (L \cdot S)$$

- Regola dell'intervallo di Landé

$$\Delta W_J = A(\alpha, L, S)\, J$$

Es. $2p^3(4S)3d\ ^5D^0_{4-0}$

	Expectated (Landé)	Measured
Δ_{10}	1800 MHz	735 MHz
Δ_{21}	3120 "	1360 "
Δ_{32}	3570 "	1594 "
Δ_{43}	2640 "	1362 "

- Hamiltoniana di Breit-Dirac
  contributi relativistici
  spin-orbita, spin-altra orbita, spin-spin
- Formula di Casimir

$$W_J = \frac{1}{2} A'(\alpha LS) + \frac{3}{8} B'(\alpha LS) \left[X(X+1) - \frac{4}{3} S(S+1) L(L+1) \right.$$

ACCURATE MEASUREMENTS OF LARGE FINE STRUCTURE SPLITTINGS

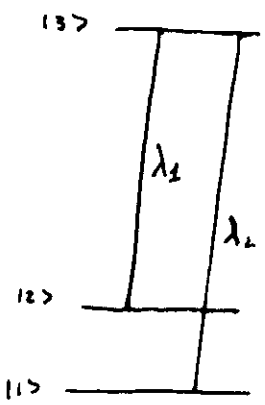

$\Delta\nu$ LARGE SPLITTING

$\Delta\nu$ > SCAN WIDTH OF THE LASER (~ 30 GHz)

$$\Delta\nu = \nu_2 - \nu_1 = c\left(\frac{1}{\lambda_2} - \frac{1}{\lambda_1}\right)$$

ABSOLUTE WAVELENGTH MEASUREM.

1. WAVEMETER
2. IODINE (+ WAVEMETER)

VISIBLE $\nu \sim 5 \cdot 10^{14}$ Hz

DOPPLER WIDTH $\Delta\nu_D \sim 10^9$ Hz

SUB-DOPPLER " $\Delta\nu_H \sim 10^7$

FREQUENCY OF THE LASER MUST BE KNOWN WITH ACCURACY

$10^{-6} \sim 10^{-8}$

IN T[illegible] RANGE ~

11[illegible]00 – 21000 [illegible]

YOU [illegible] USE I_2

SPE[illegible]UM

I_2 SPECTRUM (GOOD FOR λ CALIBRATION)

FOURIER TRANSFORM

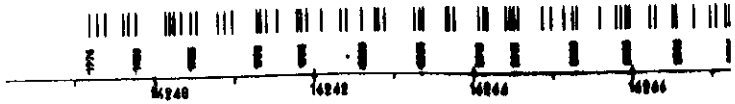

LASER DOPPLER BROAD

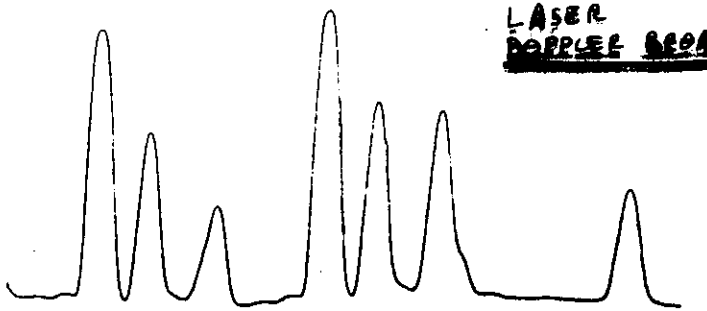

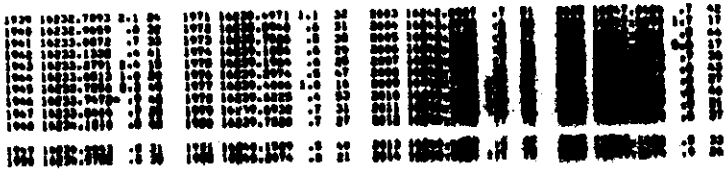

± .008 cm⁻¹

± 60 MHz

Fig. 15 [illegible]

'oppler 'profile of 6158.19 Å transitio

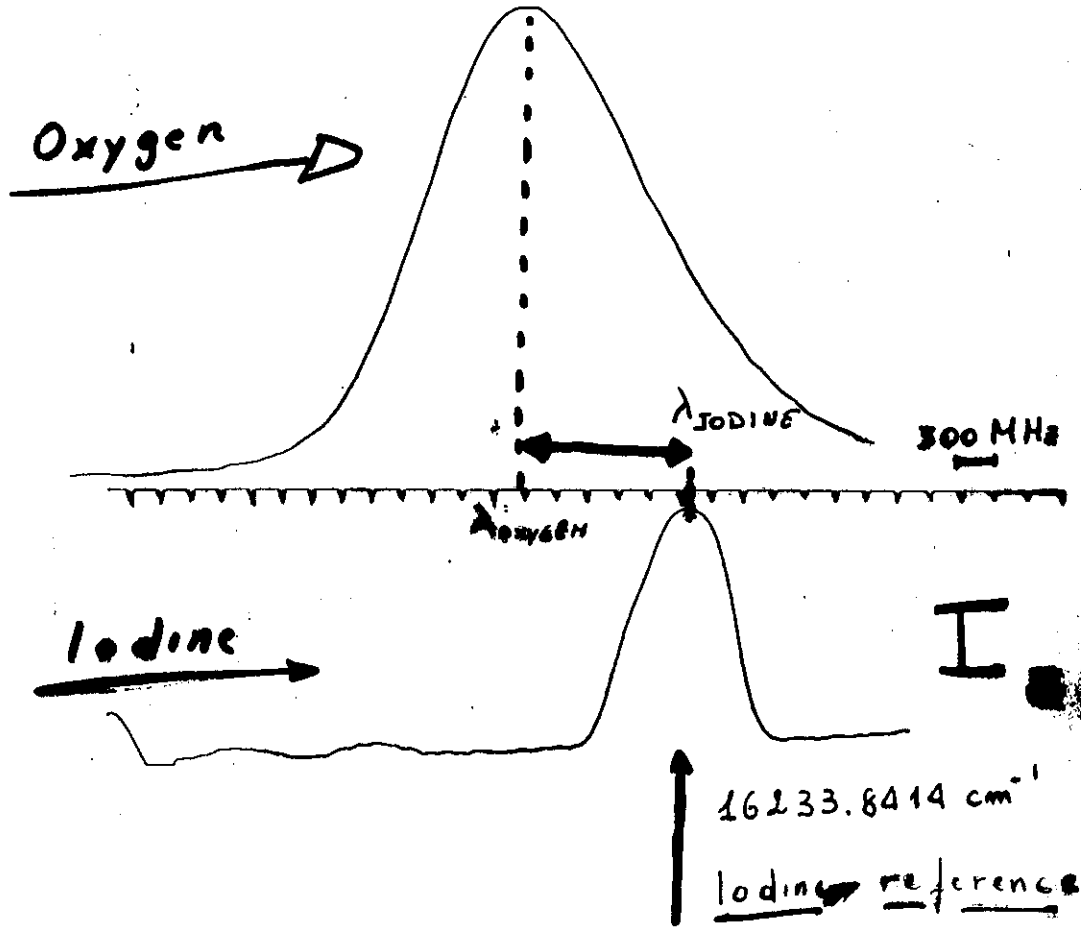

ACCURACY LIMITED BY DOPPLER WIDTH AND HF STRUCT

DOPPLER + HYPERFINE

15 comp J even ~EQUAL INTENSITY
21 comp J odd FOR J > 30

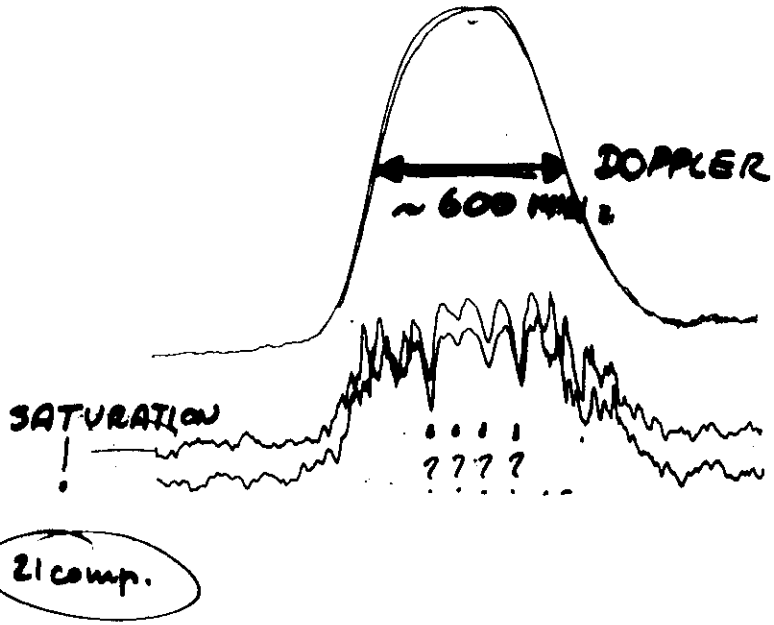

Fig. 22 Struttura iperfine delle molecole di Iodio.
Profilo di assorbimento con fascio opposto saturante.

POLARIZATION SPECTR

(SATURATION COMBINED WITH OPTICAL PUMPING).

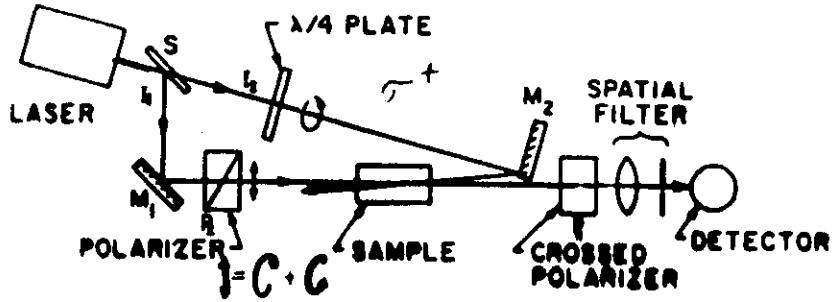

Fig.10.34. Schematic experimental arrangement for polarization spectres

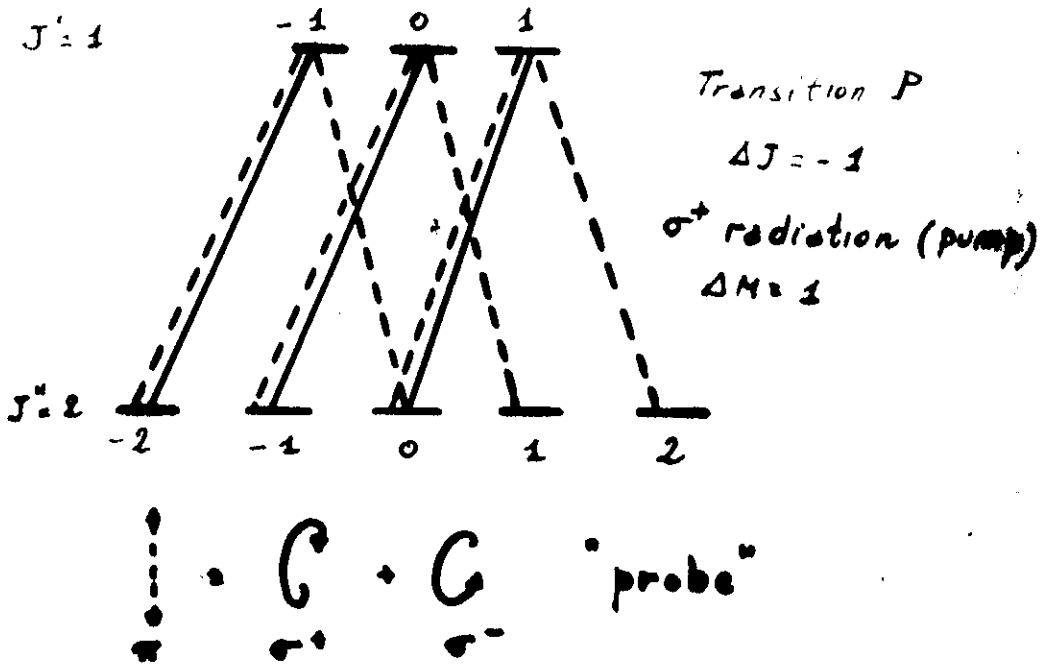

$$I_T = I_0 \left[\frac{b}{2} \Delta\alpha_0 L \frac{x}{1+x^2} + \frac{1}{4} (\Delta\alpha_0 L)^2 \frac{1}{1+x^2} \right]$$

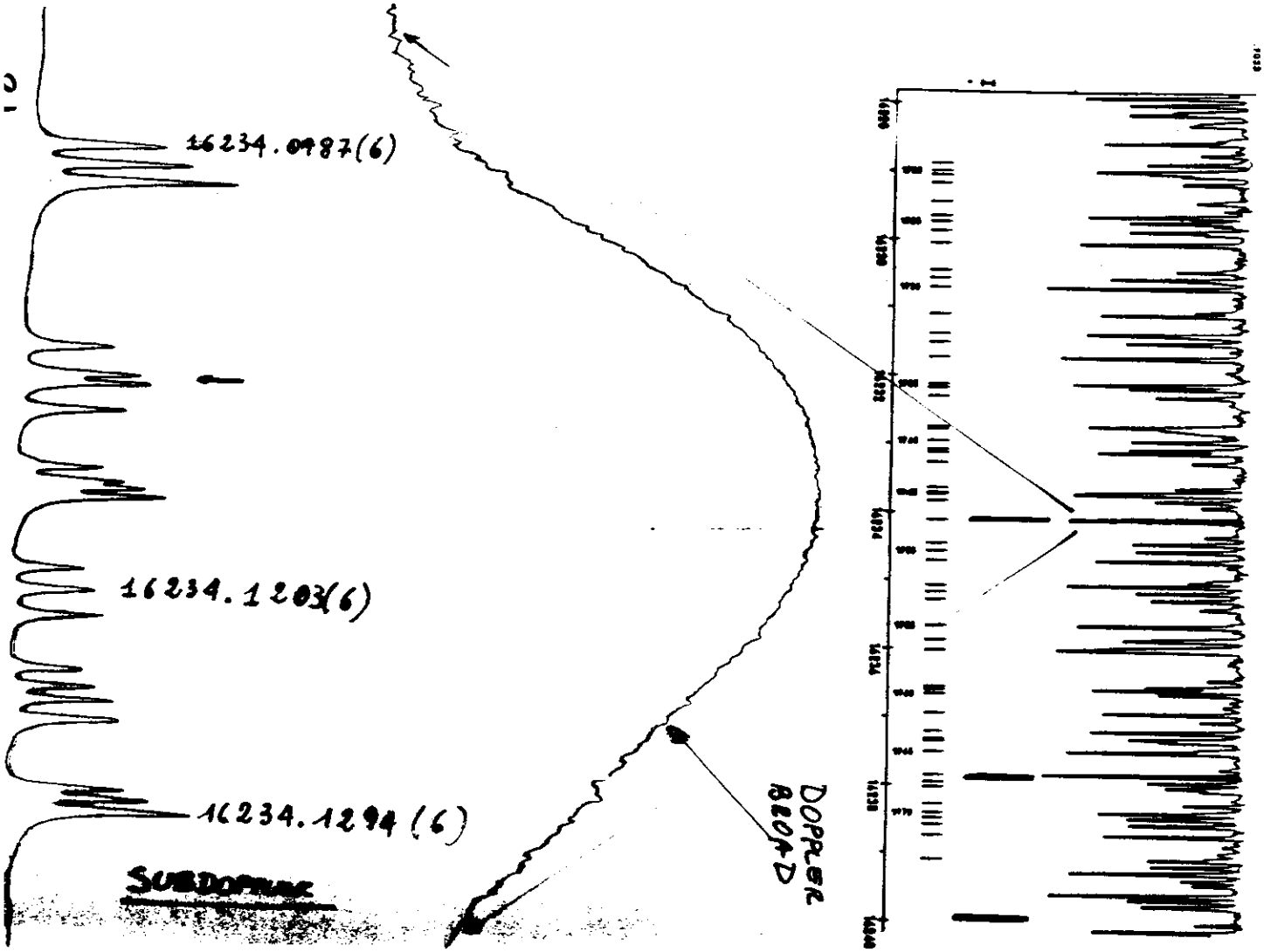

Wavemeter

$\lambda_R = 6329.906685$ Å

Accuracy : ~1 MHz

2

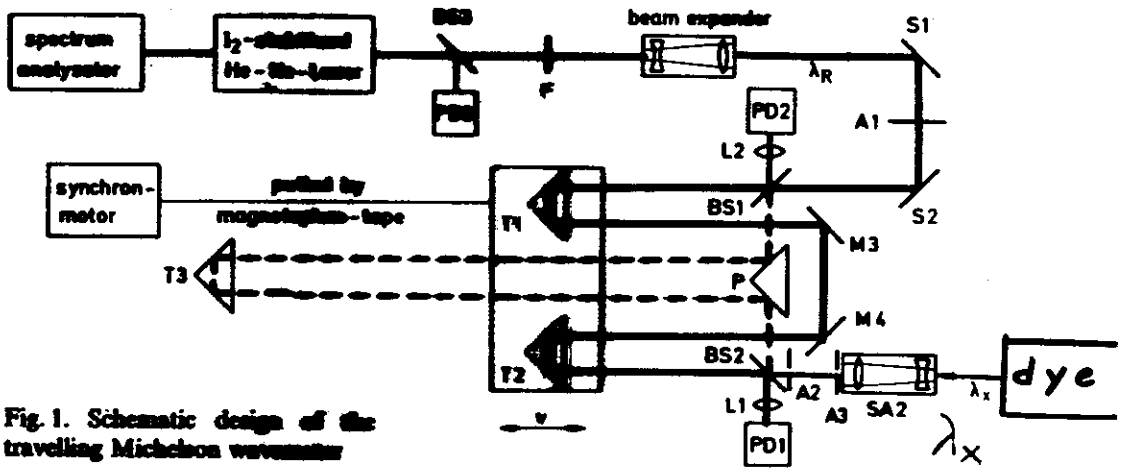

Fig. 1. Schematic design of the travelling Michelson wavemeter

$$\lambda_x = \lambda_R \cdot \frac{N_R}{N_x} \frac{n(\lambda_x, p, T)}{n(\lambda_R, p, T)}$$

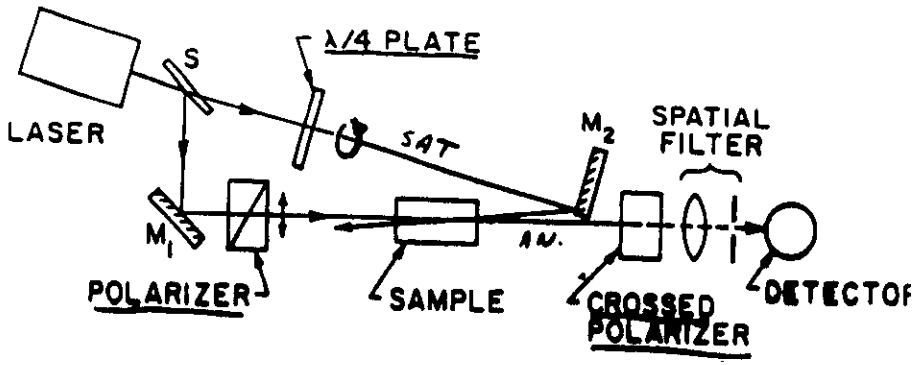

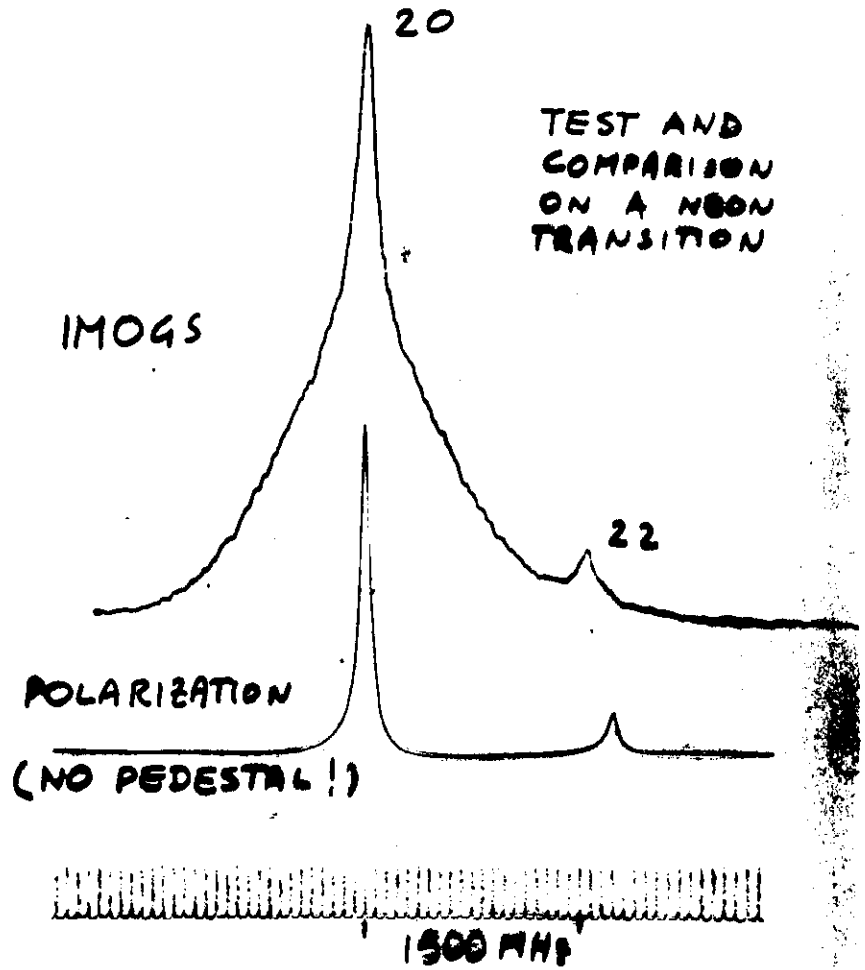

: INTERMOD. FLUORES.
: INTERMOD. OPTOGALV.
: POLARIZ. INTER. EXC.
: POLARIZ. SPECTROSCOPY

Experimental curves for the Ne $2p^5 3s\ ^3P_2 - 2p^5 3p\ ^3P_1$ transition (5882 Å), recorded with
a) IFS, discharge current (I)=150 mA, pressure (p)=0.6 torr, time constant (τ)=3 s.
b) IMOGS, I=45 mA, p=70 mtorr, τ=0.1 s
c) POLINEX, I=45 mA, p=70 mtorr, τ=0.1 s.
d) PS, I=45 mA, p=0.1 torr, τ=0.3 s.

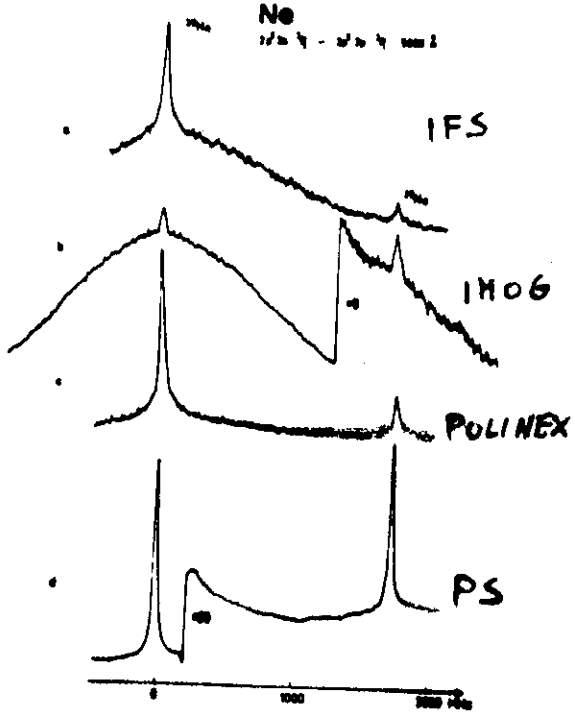

Table I

	Doppler-limited		Doppler-free			
	FS	OGS	IFS	IMOGS	POLINEX	PS
signal/noise	20	100	5	5	30	1600
signal/background	-	-	0.3	0.1	-	-

Belfrage et al. J. Phys. C7 169 (1963)

ISOTOPE SHIFTS OF OXYGEN

Three stable isotopes:

	Natural Abundance	I
^{16}O	99.76 %	0 "DOUBLY MAGIC"
^{17}O	0.03 %	5/2
^{18}O	0.21 %	0
^{15}O	unstable $\tau = 2$ min	

CLASSICAL SPECTROSCOPY INVESTIGATION

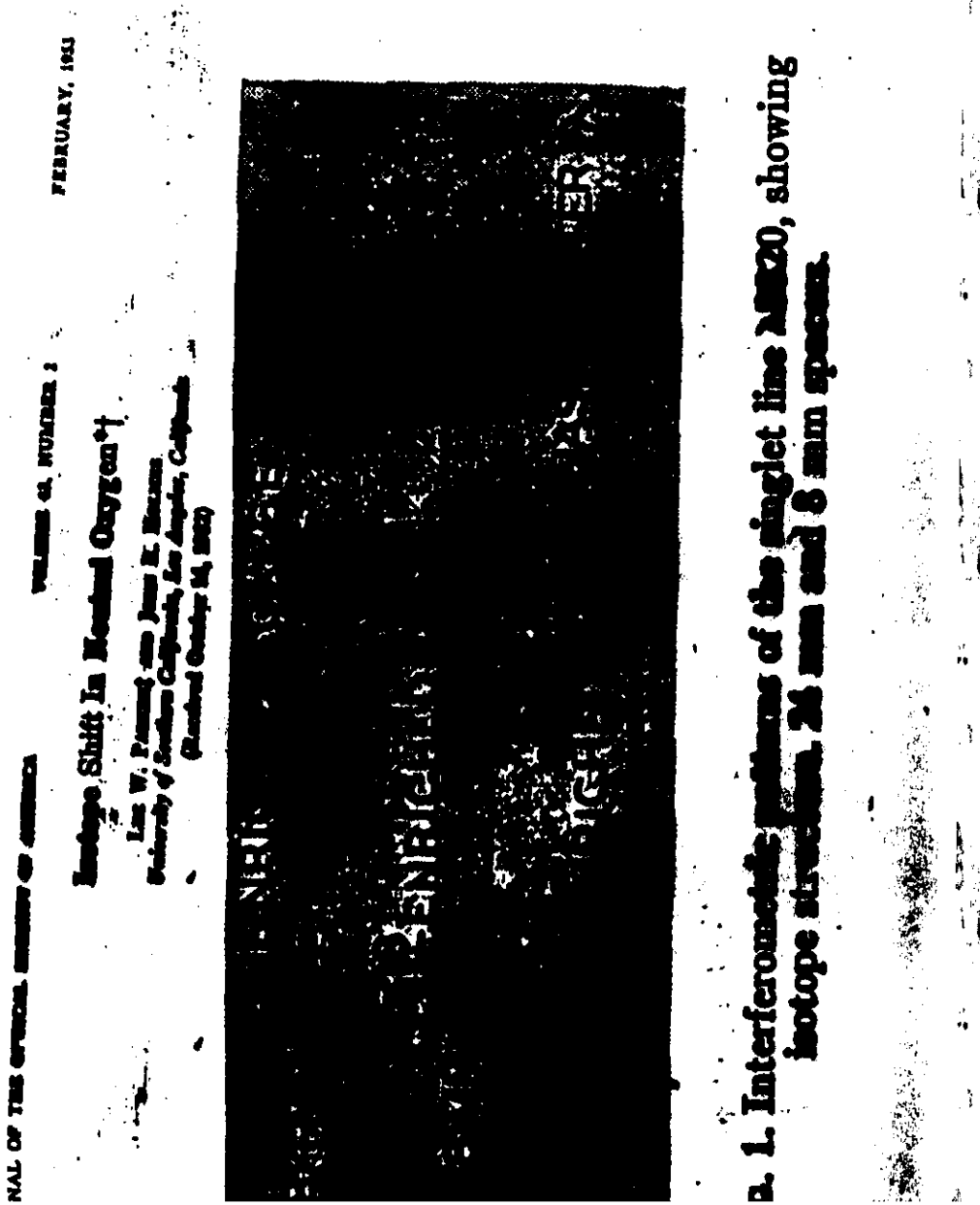

JOURNAL OF THE OPTICAL SOCIETY OF AMERICA VOLUME 42, NUMBER 2 FEBRUARY, 1952

Isotope Shift in Neutral Oxygen*†

Lee W. Parnell and John E. Mack
University of Southern California, Los Angeles, California
(Received October 24, 1951)

FIG. 1. Interferometric patterns of the singlet line λ8720, showing isotope structure. 24 mm and 8 mm spacing.

PREVIOUS MEASURES IN THE FAR-IR

+9

O

J
0
1
2

145 μm

63 μm

P. DAVIES et al (1978)

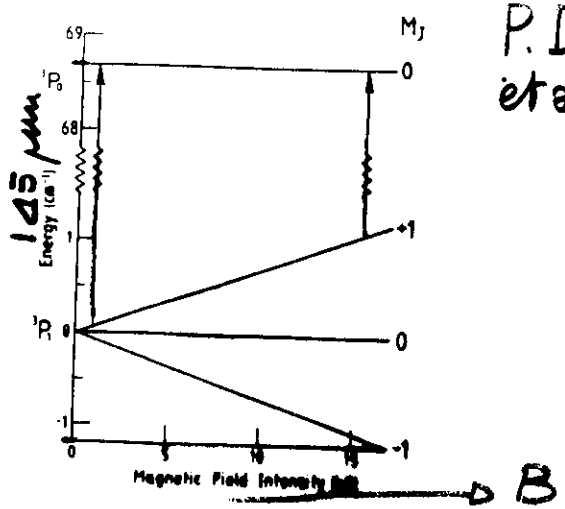

FIG. 1. LMR lines at 917 and 1068 G obtained with the CH_3OD and CH_3NH_2 lasers respectively, and their assignment to the (J, M_J) 0, 0 — 1, +1 transitions in O^3P_1.

ISOTOPE SHIFT ON $^3P_2 - {}^3P_0$

MICROWAVE DISCHARGE

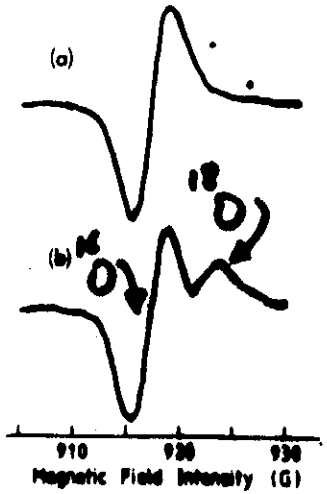

FIG. 2. LMR spectrum of $O(^3P)$ with the CH_3OD laser at 148.7 μm (a) microwave discharge in $^{16}O_2$; (b) discharge in O_2 enriched with 20% $^{18}O_2$.

natural ^{16}O

enriched (20%) ^{18}O

$$\Delta\nu = \frac{c}{\lambda}\,\frac{m(M_2 - M_1)}{(M_2 + m)(M_1 + m)}$$

6, No. 3, 1 February 1978

I.S. = 10.5 MHz

Doppler

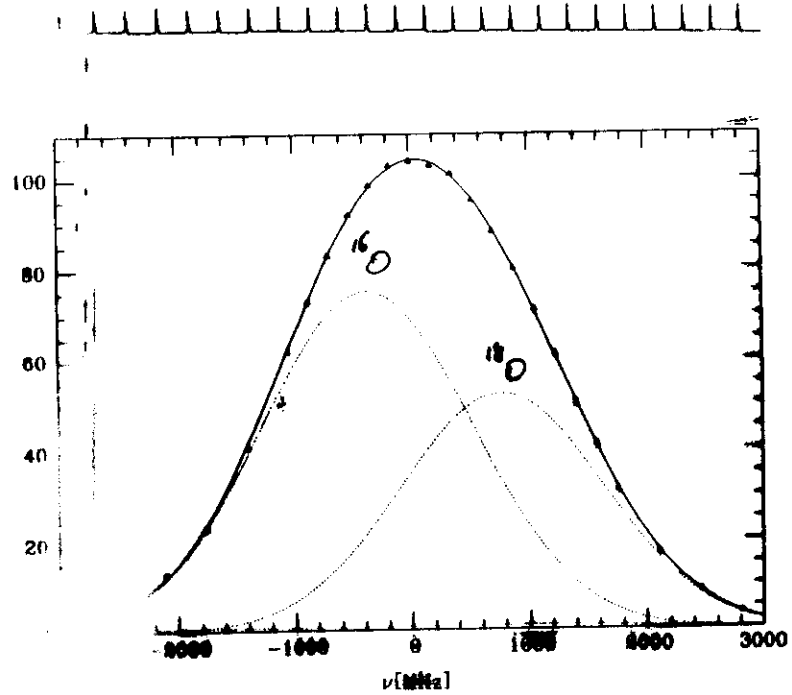

MISCELA ... ^{18}O

$3p\,{}^5P_3 - {}^2$ ... $\lambda = 6456$ Å

Miscela

Doppler

(P_{O_2} = 0.05 Torr)

(P_{Ar} = 3 Torr)

a)

^{16}O

^{18}O

Intermodulato

b)

$3p^5P_3 - 4s^5S_2$

$\lambda = 6456.4$ Å

I. S. = (1160 ± H_z

I. S.$|_{MASSA}$ = 1740

I. S.

ISOTOPE SHIFT

Isotope shift is due to two effects

$$I.S. = \left[\text{MASS EFFECT}\right] + \left[\begin{matrix}\text{VOLUME EFFECT}\\(\text{FIELD})\end{matrix}\right]$$

MASS SHIFT

$$\Delta\nu_M = \frac{\bar{P}^2_{NUCL.}}{2\,M_{NUCL.}} = \frac{1}{2M_{NUCL}}\left(\sum_{i=1}^{N}\bar{P}_i\right)^2$$

$$= \frac{1}{2M_{NUCL}}\sum P_i^{2} + \frac{1}{2\,M_{NUCL.}}\sum_{i,j}\bar{P}_i\cdot\bar{P}_j$$

↕ ↕

NORMAL MASS SHIFT NMS

SPECIFIC MASS SHIFT SMS

↕ ↕

$$\Delta\nu_{NMS} = \frac{c}{\lambda}\,m_e\,\frac{(M_2 - M_1)}{M_2\cdot M_1}$$

"difficult" to calcul. Harthree. Fock approach + pertub."

Z atomic numb

A mass number

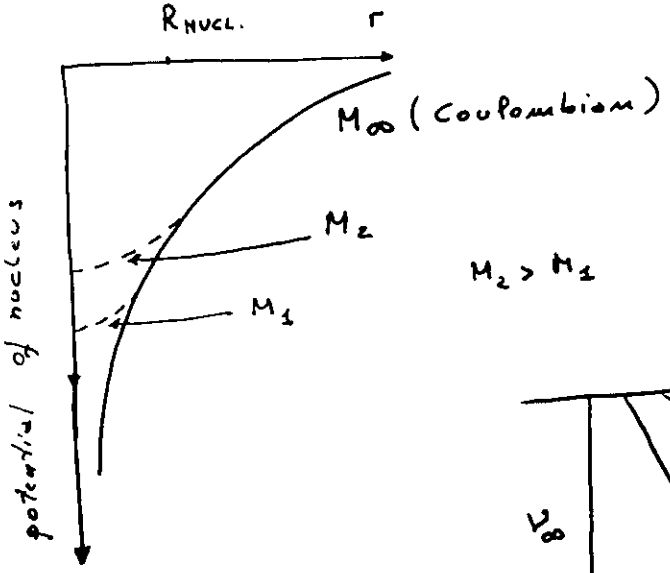

$$R_{NUCL} \propto \sqrt[3]{A}$$

$M_2 > M_1$

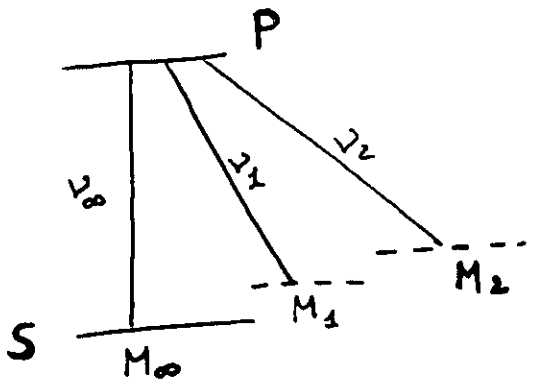

. S orbital are more penetrating

. For heavier nucleus electron is less bounded.

Volume effect is negligible for light atoms;

... negligible for $A > 60$

KING-PLOT REPRESENTATION

RESIDUAL SHIFT = TOTAL SHIFT −

NORMAL MASS SHIFT

= SPECIFIC MASS SHIFT +

VOLUME SHIFT

It can be shown that

α, β isotopes

"d" transition

$$\Delta\nu_R = \Delta\nu_{RMS} + \Delta\nu_{VS}$$

$$= K^d \cdot A_{\alpha\beta} + E^d C_{\alpha\beta}$$

where

$$K^d \propto \sum \bar{P}_i \cdot \bar{P}_j \qquad A_{\alpha\beta} = \frac{A_\beta - A_\alpha}{A_\beta A_\alpha}$$

$$E^d \propto |\psi(0)|^2 \qquad C_{\alpha\beta} \propto \langle r^2 \rangle_\beta - \langle r^2 \rangle_\alpha$$

KING PLOT

MODIFIED SHIFT

$$\mu^a_{\alpha\beta} = \frac{\Delta\nu^a_{\alpha\beta}}{A_{\alpha\beta}} = \Delta\nu^a_{\alpha\beta}\,\frac{A_\alpha A_\beta}{A_\beta - A_\alpha}$$

$$\mu^a_{\alpha\beta} = K^a + E^a\,\frac{C_{\alpha\beta}}{A_{\alpha\beta}} \qquad (1)$$

$$\mu^b_{\alpha\beta} = K^b + E^b\,\frac{C_{\alpha\beta}}{A_{\alpha\beta}} \qquad (2)$$

By combining eq. (1) and (2) we have:

$$\mu^a_{\alpha\beta} = \frac{E^a}{E^b}\,\mu^b_{\alpha\beta} + \left(K^a - K^b\frac{E^a}{E^b}\right)$$

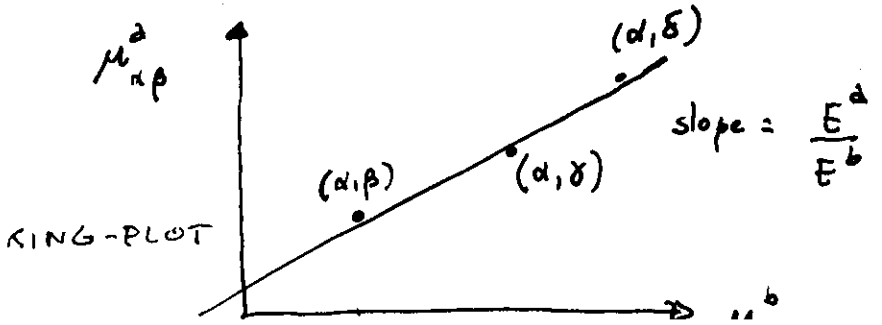

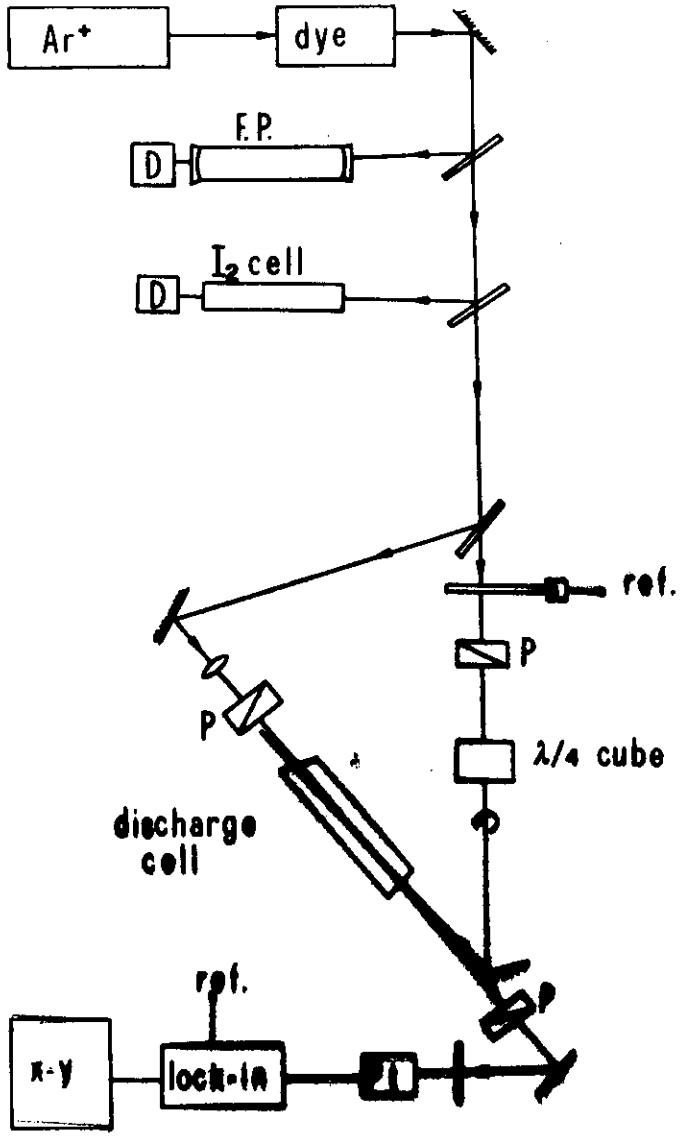

Experimental set-up for polarization spectroscopy

4^5D $\lambda = 615.8$ nm

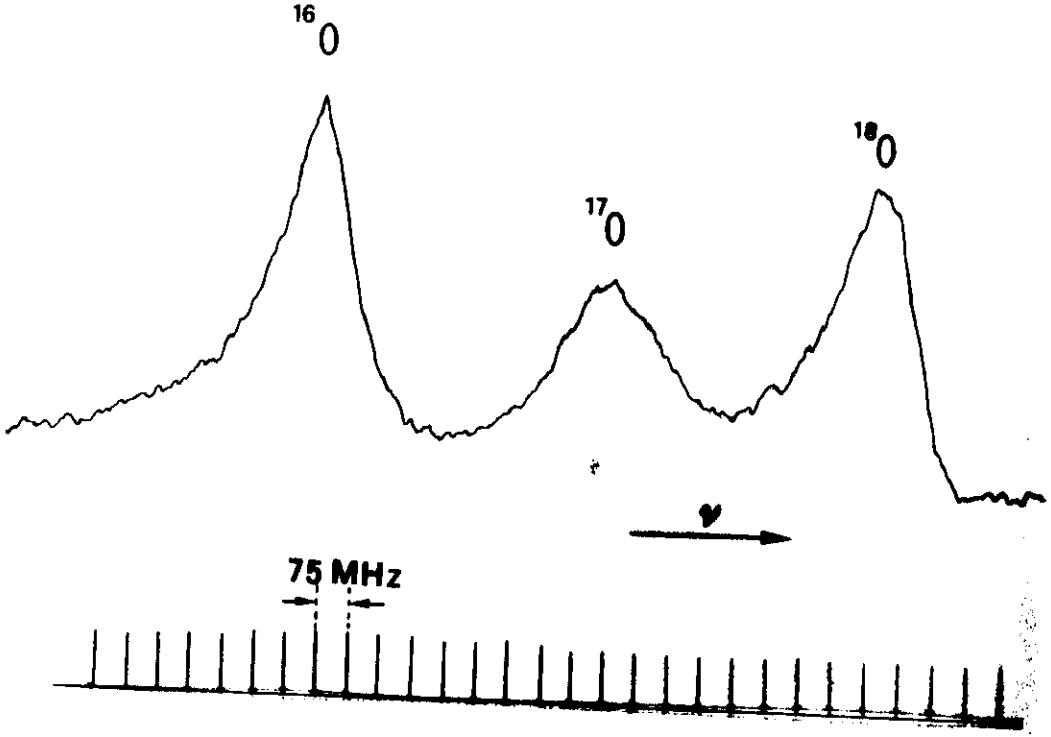

fig.8.3. Registrazione della transizione $3p^5P_3 \rightarrow 4d^5D_4$ dei tre isotopi dell'ossigeno. Scarica a radiofrequenza 1.2 torr di Ar e 0.08 torr di O_2.

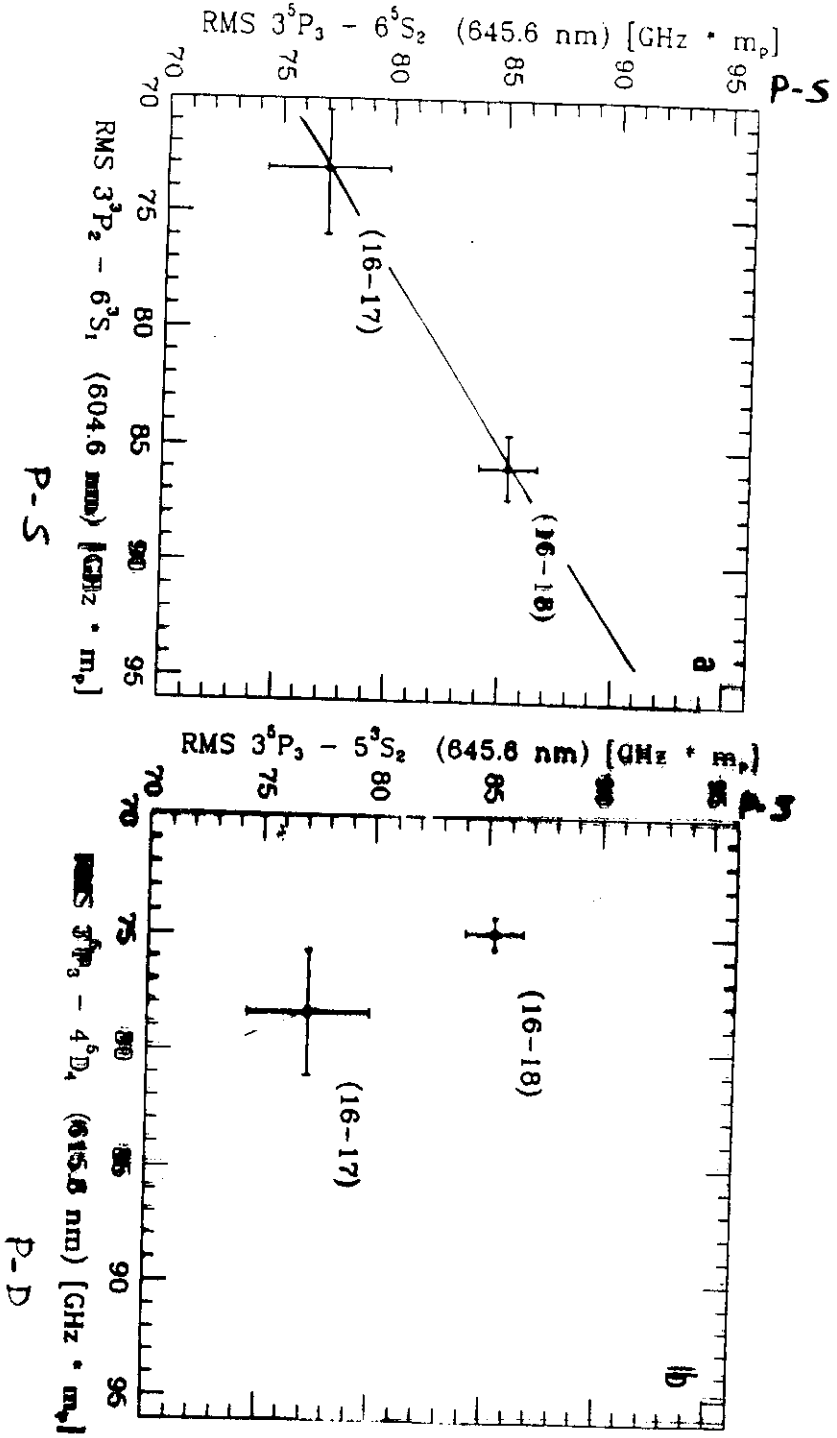

Nuclei "Magici"

	(82)
$1h_{11/2}$	
$2d_{3/2}$	
$3s_{1/2}$	
$2d_{5/2}$	
$1g_{7/2}$	
	(50)
$1g_{9/2}$	
$2p_{1/2}$	
$2p_{3/2}$	
$1f_{5/2}$	
	(28)
$1f_{7/2}$	
	(20)
$1d_{3/2}$	
$2s_{1/2}$	
$1d_{5/2}$	
	(8)
$1p_{1/2}$	
$1p_{3/2}$	
	(2)
$1s_{1/2}$	

INTEREST FOR ISOTOPE SHIFT INVESTIGATION OF LIGHT ELEMENTS

"MAGIC" NUCLEI

SHIFT = NORMAL MASS + SPECIFIC MASS + FIELD EFFECT

Ni *

^{40}Ca * *

^{16}O * *

^{4}He * *

^{16}O : 99.76 % ^{17}O : 0.03 % ^{18}O : 0.20 %

L.E. Parker and J.R. Holmes
J. Opt. Soc. Am. 43, 103 (1953)

Transition	Wavelength (nm)	Isotopic shift (present work) (mK)	Previous data [9] (mK)
$3p\ ^5P_3 - 4d\ ^5D_4$	615.8	1000 (40)	< 600
$3p\ ^5P_2 - 5s\ ^5S_2$	645.5	1000 (20)	—
$3p\ ^5P_3 - 5s\ ^5S_2$	645.6	1000 (20)	< 600
$3p\ ^3P_2 - 6s\ ^3S_1$	604.6	1000 (40)	—

DIODE LASER

- WIDE SPECTRAL RANGE $0.6 \div 0.9\ \mu m$
  $1.3 \div 1.6\ \mu m$
  $2 \div 30\ \mu m$
- LOW NOISE
- TUNABILITY (λ (Temperature, pressure, current)
- BAND WIDTH 10 KHz — 10 MHz
- POWER $\approx$ 10 mW
- ELECTRICAL POWER $\approx$ 100 mW
- CHEAP
- SMALL SIZE

OXYGEN

TRIPLETS QUINTETS

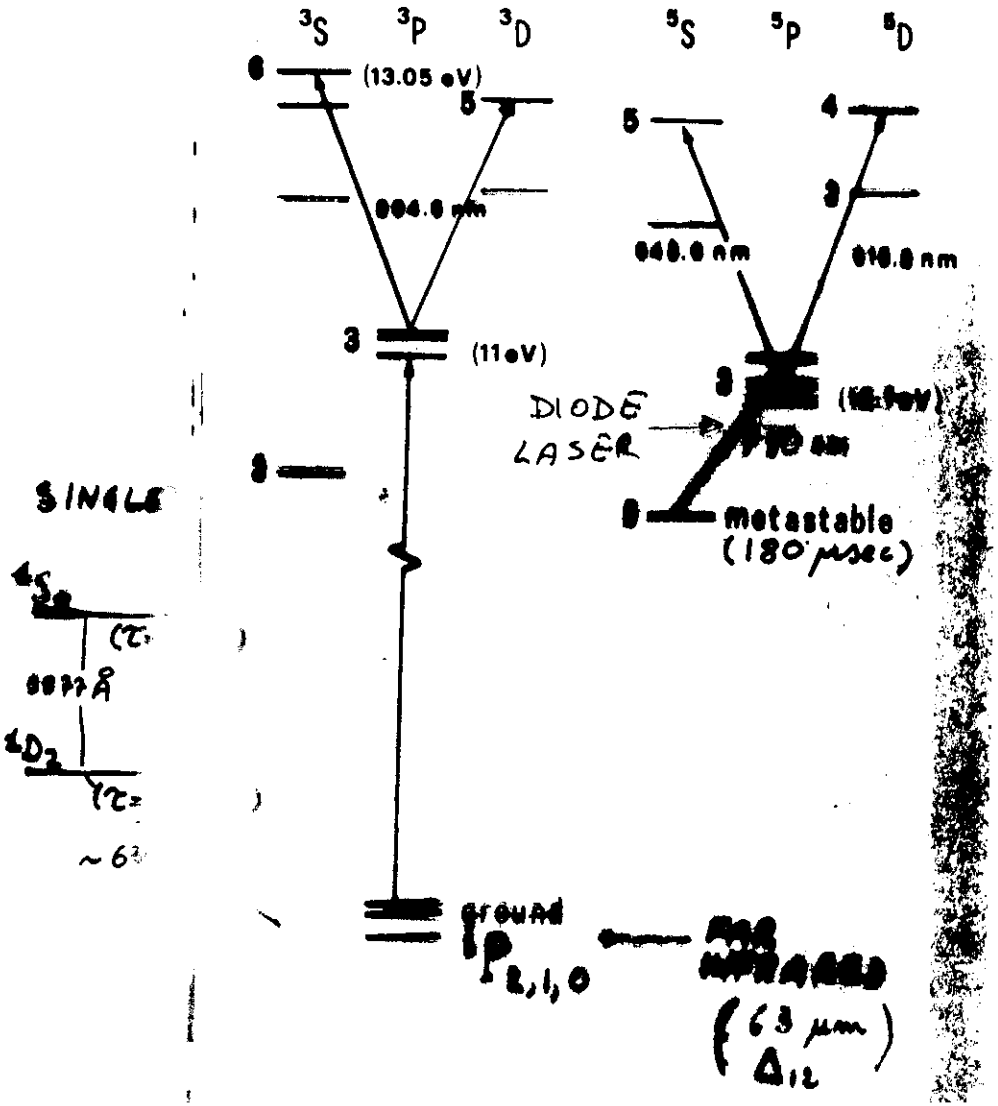

SINGLE

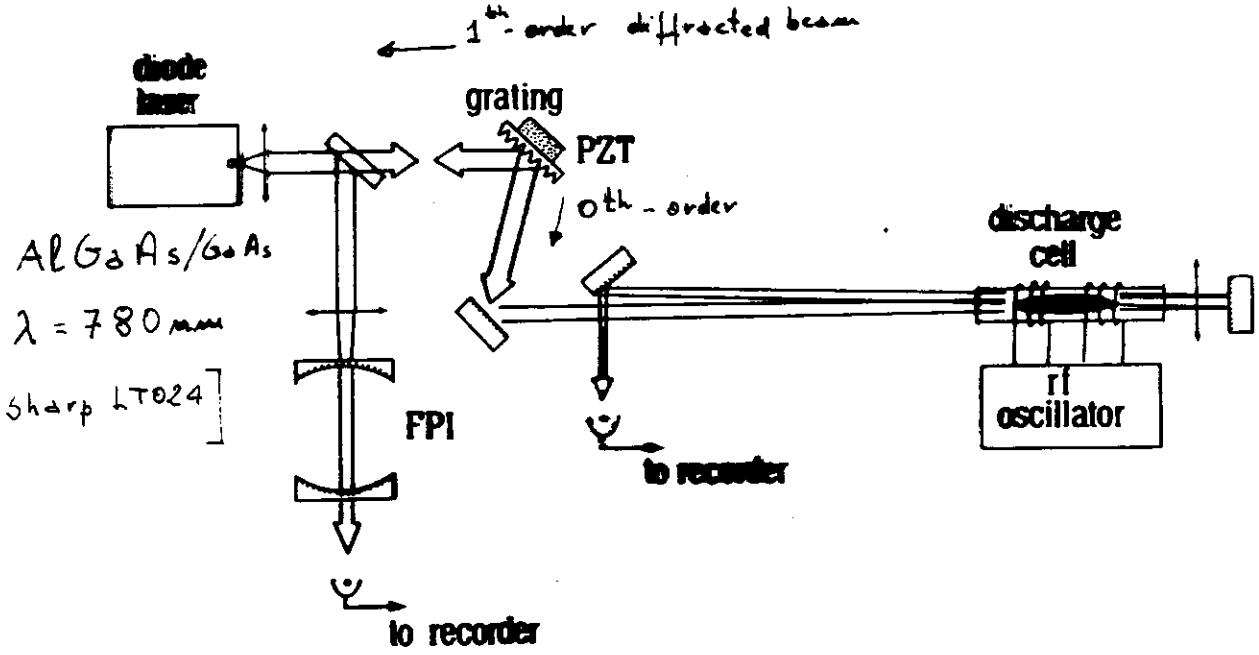
1th - order diffracted beam
diode laser
grating
PZT
0th - order
discharge cell
AlGaAs/GaAs
λ = 780 nm
Sharp LT024
FPI
rf oscillator
Io recorder
Io recorder

Fig. 2

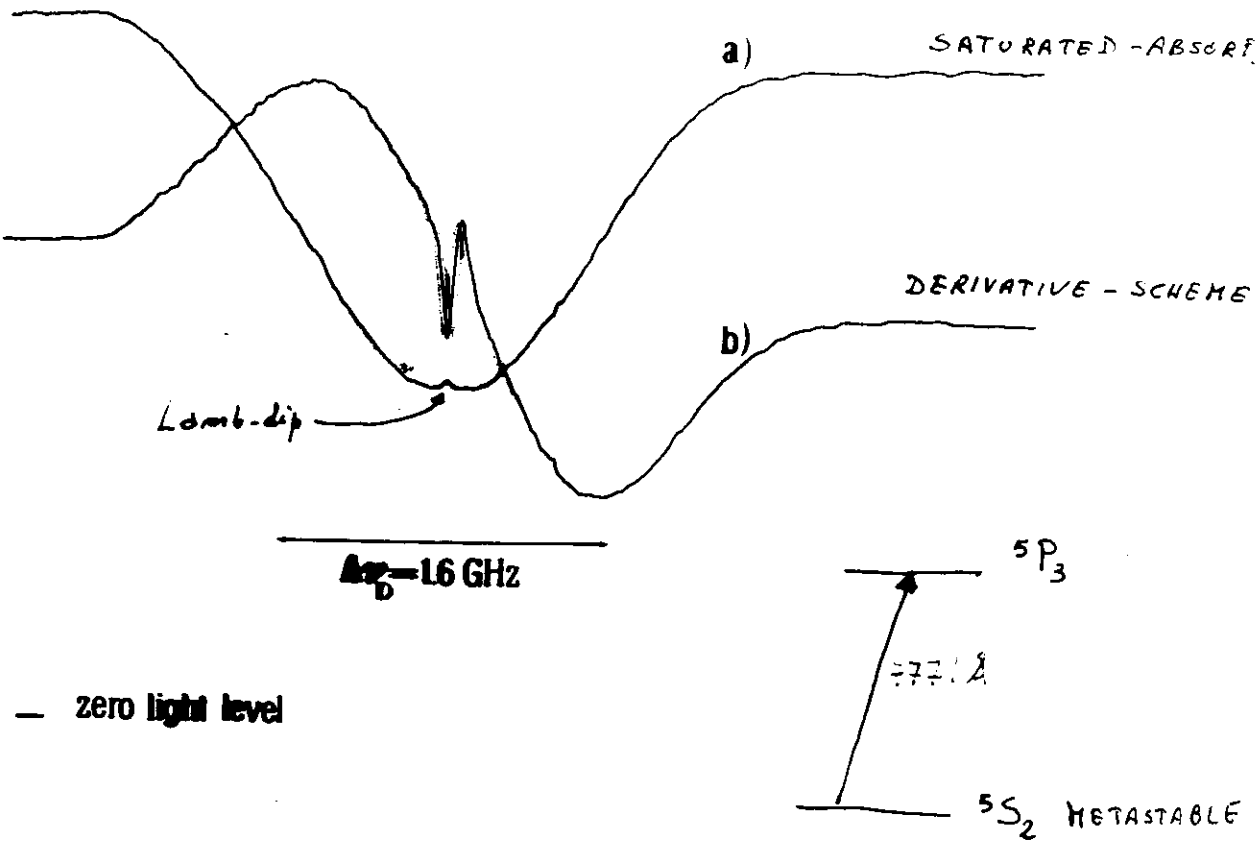
a)
SATURATED - ABSORP.
DERIVATIVE - SCHEME
b)
Lamb-dip
Δνhfs = 1.6 GHz
zero light level
5P3
7721 Å
5S2 METASTABLE

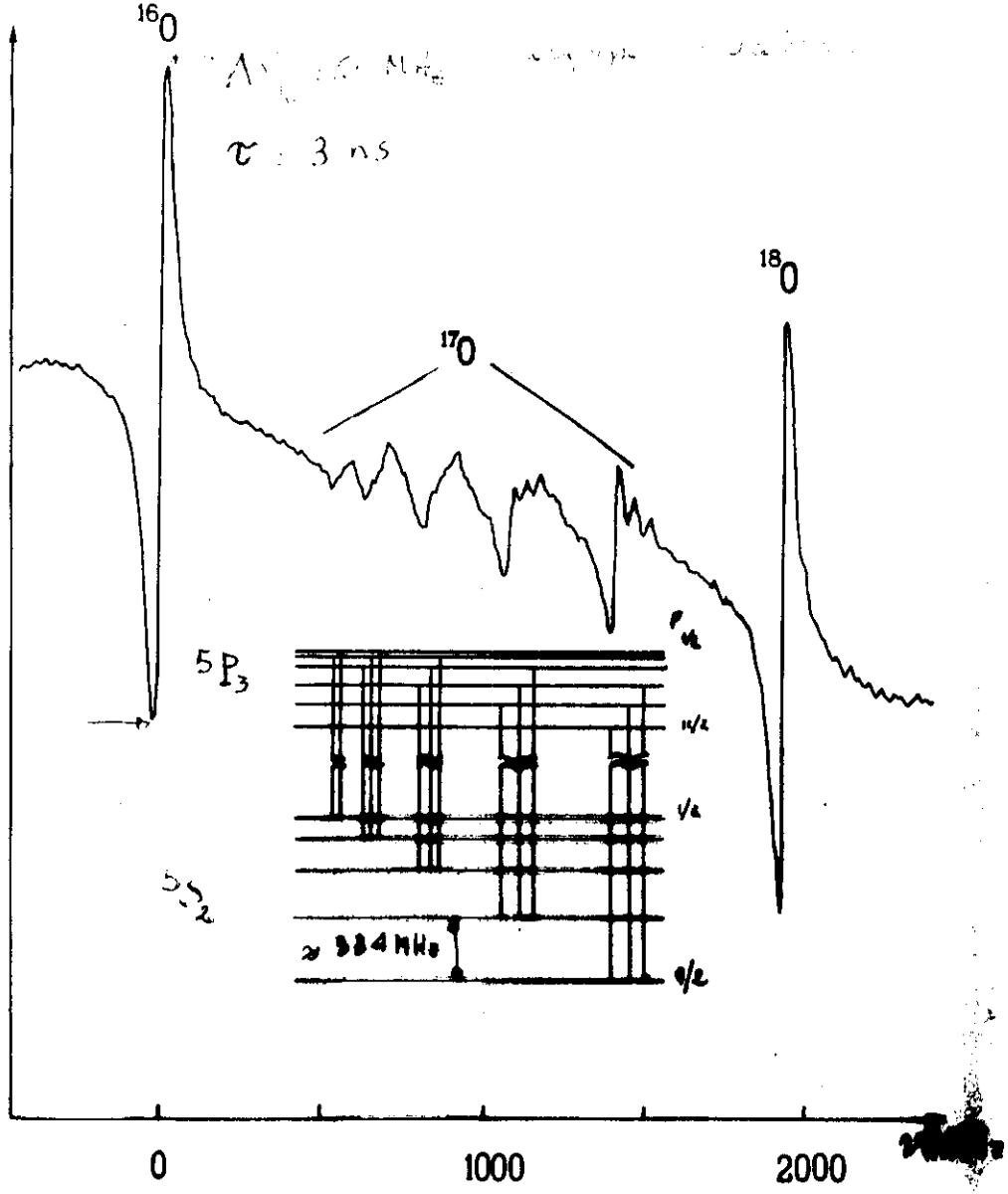

HFS constant $A = 74.3(2)$ MHz

LASER [illegible] OF [illegible] OXYGEN

$v \simeq 10^5$ cm/s

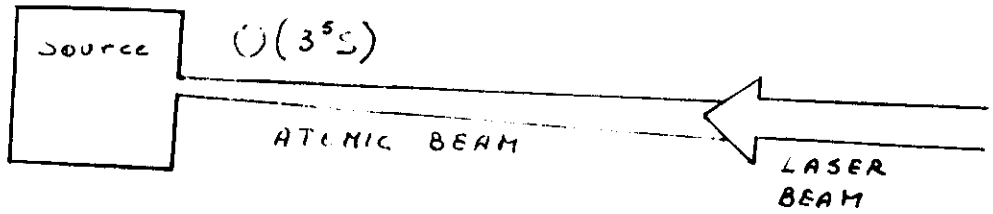

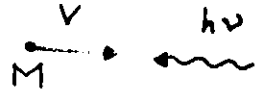

$\Delta V = \frac{h\nu}{\epsilon M}$

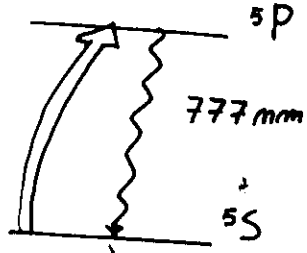

$N_{cycl} \simeq 45000$

$\tau_{cooling} \simeq .27$ ms

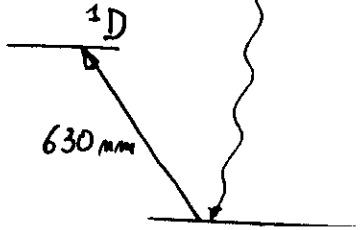

Advantages

- CLOSED TRANSITION
- "COLD" ATOMS IN THE GROUND STATE

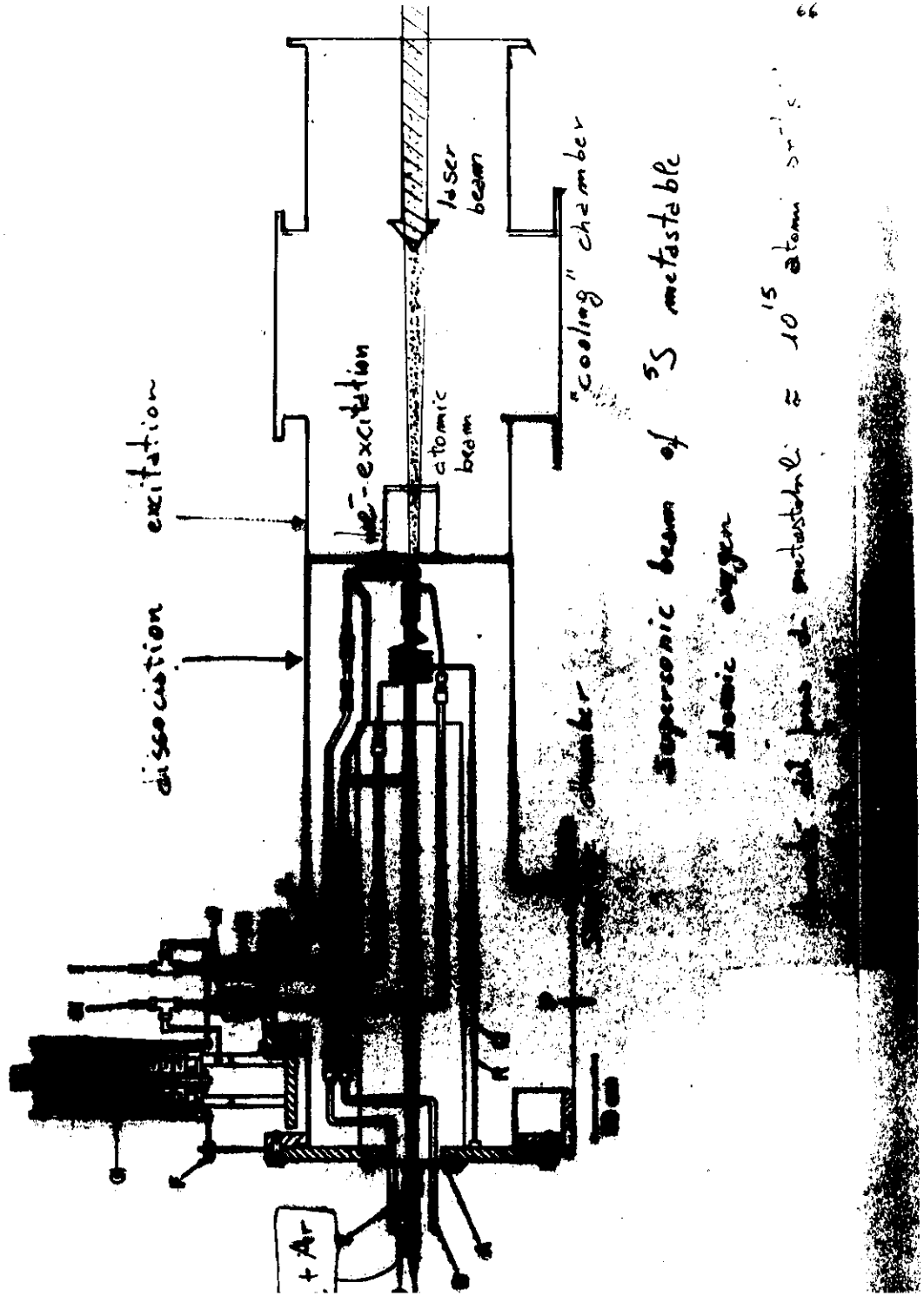

SPECTROSCOPY OF REFRACTORY ELEMENTS :

Calcium : Ca , Ca^+

Titanium : Ti , Ti^+

Interesting for :

astrophysics

metrology

Production : hollow cathode discharge

"Sputtering"

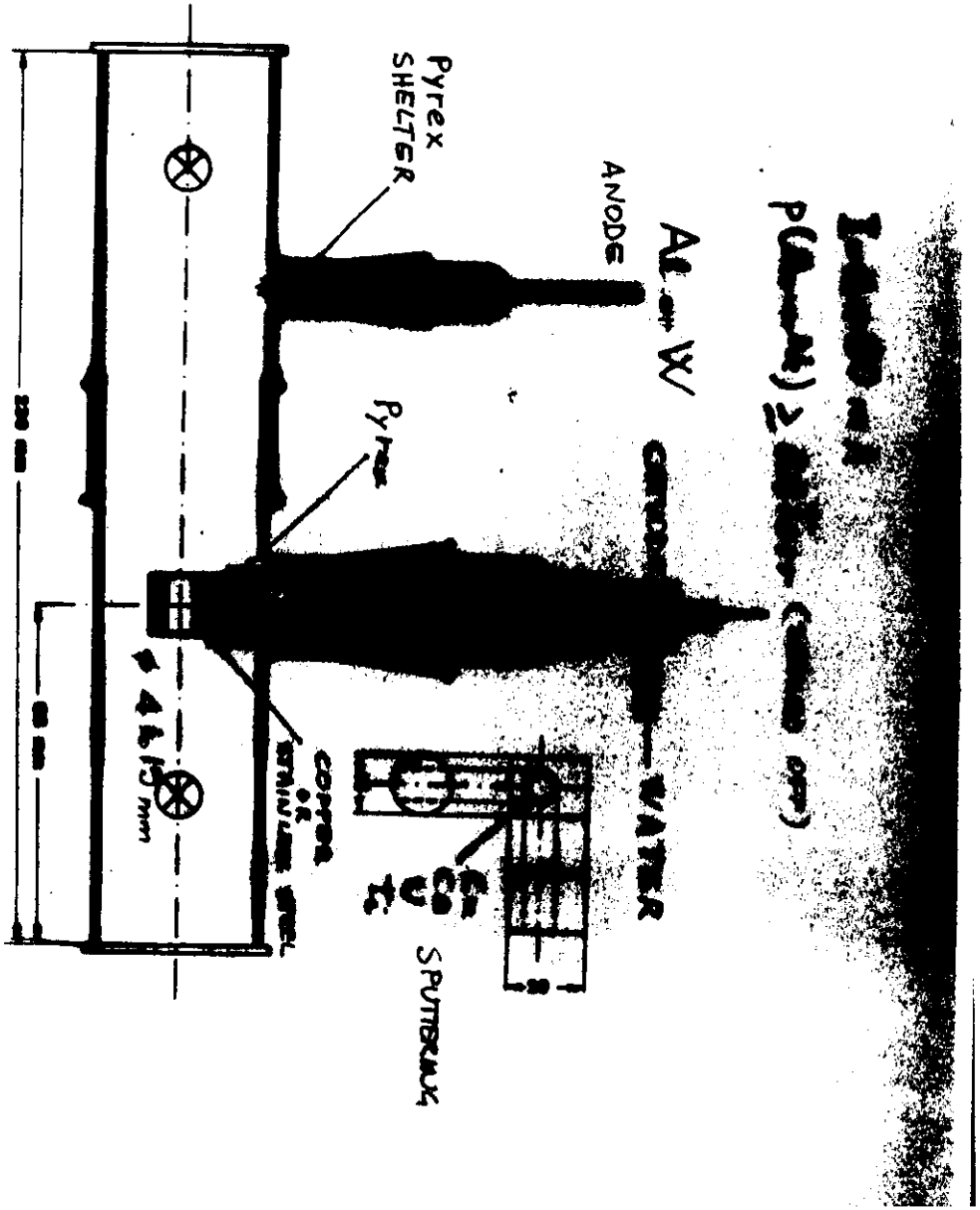
Pyrex
SHELTER
ANODE
Al or W
Pyrex
WATER
SPUTTERING

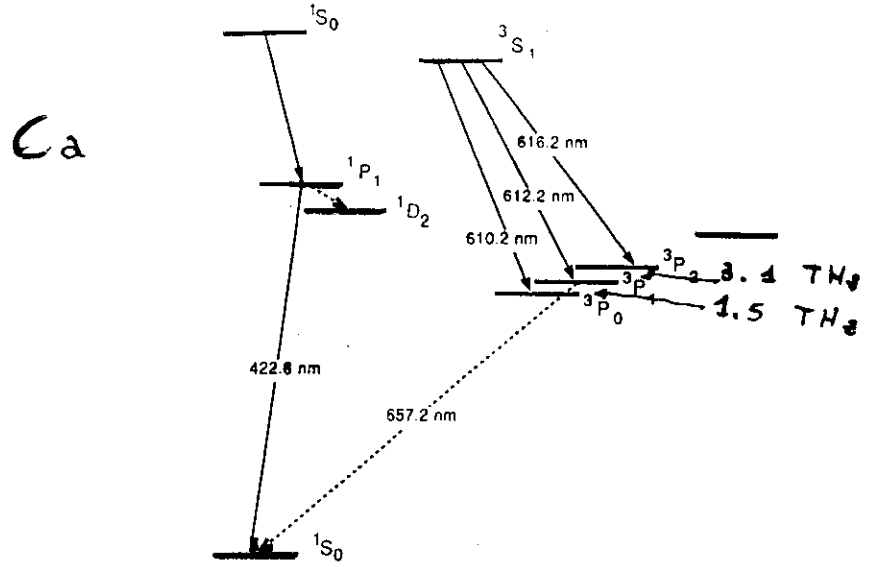
Ca
$^1S_0$
$^3S_1$
616.2 nm
612.2 nm
610.2 nm
$^1P_1$
$^1D_2$
$^3P_2$
$^3P_1$
$^3P_0$
3.4 THz
1.5 THz
422.8 nm
657.2 nm
$^1S_0$

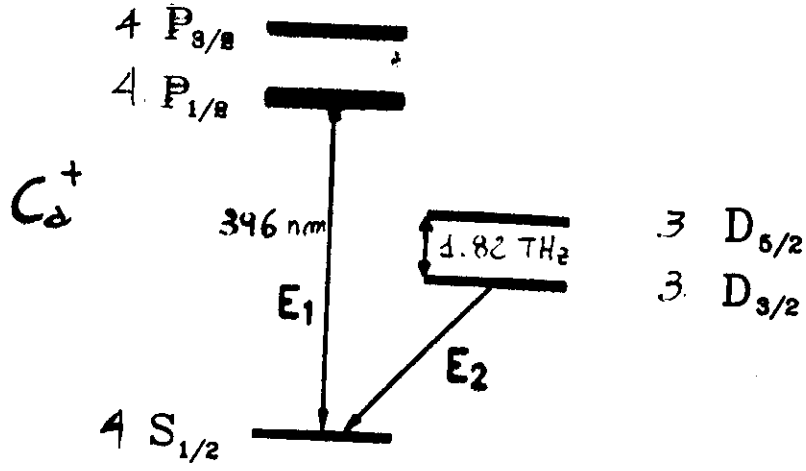
Ca^+
4 $P_{3/2}$
4 $P_{1/2}$
396 nm
E_1
1.82 THz
E_2
4 $S_{1/2}$
3 $D_{5/2}$
3 $D_{3/2}$

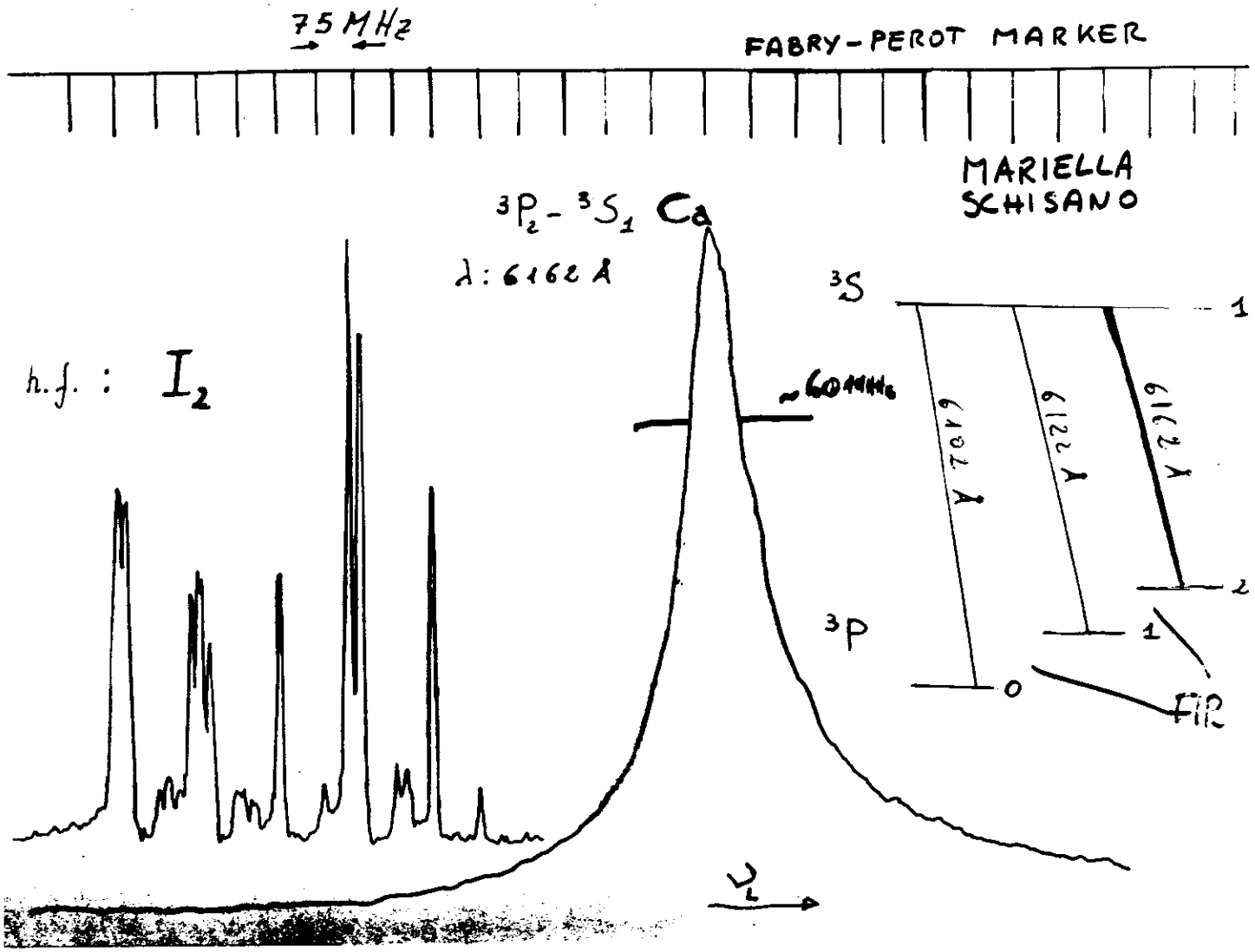
75 MHz
FABRY-PEROT MARKER
MARIELLA SCHISANO
$^3P_2 - ^3S_1$ Ca
λ: 6162 Å
h.f. : I_2
~60 mK
^3S
^3P
6102 Å
6122 Å
6162 Å
1
2
1
0
fig

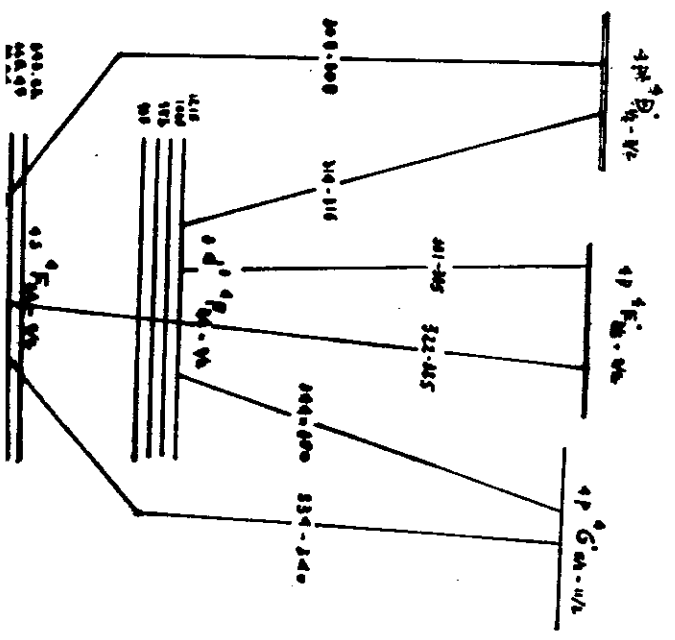

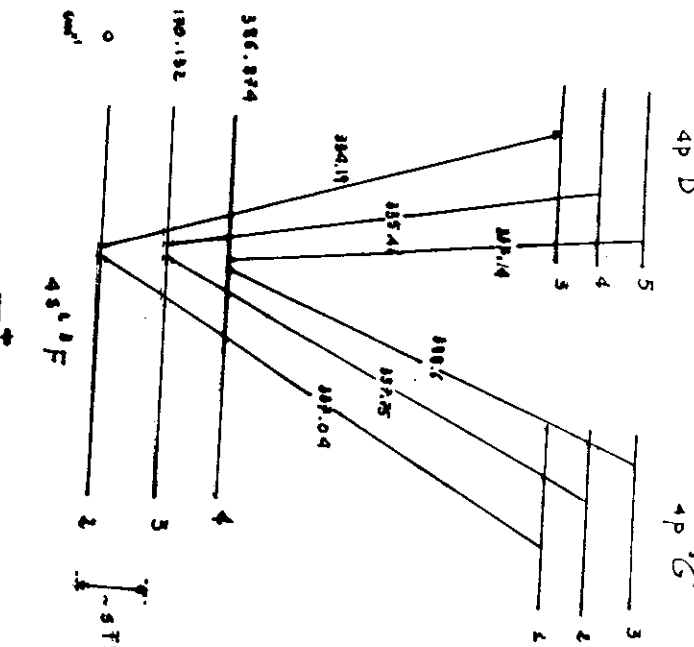
$4p\ ^3D_1$
$4p\ ^3G_3$
$4s\ ^3F_2$

Titane : $4^3F_2 - 4p^3D^\circ_3$ λ : 334.14 nm